DESIGN OF A NOVEL ANNULAR RECESS ELECTRODE FOR RESISTANCE SPOT WELDING

BY

MUWANGA GODFREY FRED

(B.Eng. Mech & Manuf. Eng, KYU)

18/U/19352/GMSE/PD

A DISSERTATION SUBMITTED TO THE DIRECTORATE OF RESEARCH AND GRADUATE TRAINING IN PARTIAL FULFILMENT OF THE REQUIREMENTS FOR THE AWARD OF THE DEGREE OF MASTER OF SCIENCE IN ADVANCED MANUFACTURING SYSTEMS ENGINEERING OF KYAMBOGO UNIVERSITY

OCTOBER, 2024

DECLARATION

I, Muwanga Godfrey Fred, hereby declare that this dissertation is my original work and has never been presented to any university or institution for any academic award.

Sign: ..... Date: .....

30/09/2024

DEDICATION

I dedicate this dissertation to the following; Ms Nabi Oki for supporting me with tuition fees, my wife Sarah Nakanjako and the entire family whose unwavering support has been a source of inspiration and strength throughout my research journey. May the almighty God bless and reward you abundantly.

ACKNOWLEDGEMENT

I would like to express my sincere appreciation for the invaluable support and guidance I received during the course of my research at the Department of Mechanical and Manufacturing Engineering, Kyambogo University. I am deeply grateful to my supervisors, Dr. Samuel Kangwagye, and Dr. Maureen Ssempijja, for their unwavering assistance throughout the entirety of my work.

I extend my heartfelt thanks to the Executive Director, of Uganda Industrial Research Institute (UIRI), the Managing Director of Roofings Group of companies and Managing Director Sun Maker, Heads of departments metal machining and welding shops at Nakawa Vocational Training College for allowing me access to their facilities and using the equipment to carry out my research work.

Special gratitude is extended to Prof. Titus Watmon Bitek whose unwavering support has been a source of strength throughout my research journey.

Muwanga Godfrey Fred

TABLE OF CONTENTS

LIST OF TABLES

LIST OF FIGURES

LIST OF ABBREVIATIONS AND ACRONYMS

RSW	Resistance Spot Welding
NDPIII	National Development Plan III
NPA	National Planning Authority
UBOS	Uganda Bureau of Statistics
HAZ	Heat-Affected Zone
SDG	Sustainable Development Goal
ANOVA	Analysis of variance
ASS	Austenitic Stainless Steel
S/N	Signal to Noise
KVA	Kilo Volt Ampere
KN	Kilo Newton
KV	Kilo Volts

ABSTRACT

The effectiveness and longevity of resistance spot welding (RSW) hinge significantly on the geometry of welding electrodes, a critical factor influencing weld characteristics and electrode lifespan. Achieving an optimal electrode design requires a delicate balance between electric current density distribution and thermal-mechanical stiffness. However, improving one aspect often comes at the expense of the other. This study addresses this challenge by proposing an innovative electrode design featuring an annular recess filled with a refractory material. In electrode design, the well-established trade-off between current density distribution and thermal-mechanical stiffness is crucial. Neglecting either factor welding current or nugget diameter can result in accelerated wear and compromise the integrity of the weld. It underscores the importance of considering both elements to ensure optimal weld quality and performance. The novel electrode design with an annular recess aims to strike a harmonious balance between these competing considerations. This research hypothesizes that such a design configuration has the potential to yield stronger weld joints. The primary objective of this study is to design an electrode that would ensure optimal weld quality and performance. To achieve this, resistance spot welding parameters are identified and optimized. By delving into the intricacies of this innovative electrode design, the research endeavours to offer valuable insights for improving the overall performance and longevity of resistance spot welding processes.

CHAPTER ONE: INTRODUCTION

The chapter introduces a background to the study on this method of metal joining, a statement of the problem, and the objectives of the study. It states the general, specific objectives and, justification for the study. It also provides an understanding of how the study will be undertaken.

1.1 Background

Industries and consumers face increasing pressure to mitigate greenhouse gas emissions resulting from manufacturing processes and product usage to combat global warming effects, (Forster et al., 2023). The automotive sector, a major contributor to these emissions, has responded by prioritizing measures such as enhanced fuel efficiency, weight reduction in products, and the integration of alternative fuel engines, (Ghatei-Kalashami et al., 2022). Achieving reduced vehicle weight involves innovative designs and the use of materials with high strength-to-weight ratios, including high-strength steels, aluminum, or composite materials, (Tisza & Czinege, 2018). While these solutions contribute to emission reduction, they bring about manufacturing challenges due to the novel and intricate nature of components and materials. Joining technology is important in modern manufacturing, and the characteristics of joints formed significantly impact on overall product performance. The growing complexity of vehicle products poses challenges for joining technologies. In the realm of RSW, this thesis emphasizes the importance of process planning, focusing on optimizing process parameters for product development, process efficiency, and overall cost-effectiveness. The progression of process planning highlights the need to optimize a specific set of materials, equipment,

and applications with corresponding process parameters to achieve satisfactory welding outcomes. This is shown in Figure 1.1 below.

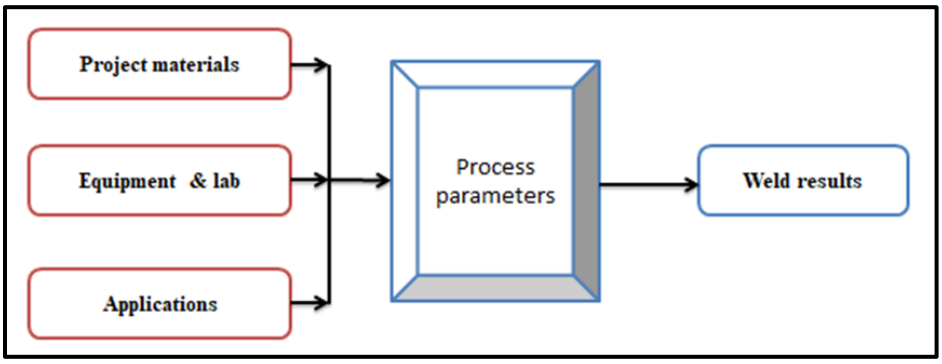

Figure 1.1: Illustration of progression of process planning

RSW stands out as popular among the various welding methods, (Tanmoy, 2022). Its notable attributes, such as rapid welding speeds and the inherent ability of electrodes to automatically clamp, render it a highly suitable process for automated and high-production settings, (Biradar & Dabade, 2020). It is commonly and widely used in joining metal sheets in most automotive manufactories, (Ghatei-Kalashami et al., 2022). In the process, the joint is positioned between two copper electrodes in the machine, and these electrodes can be swapped for different applications. The electrodes come together, compressing the sheets. Subsequently, current is automatically activated for a predetermined duration, leading to melting at the interface. A transformer supplies the current, which can reach up to 50,000 Amperes at a low voltage ranging from about 4 to 25 Volts, (Bamberg et al., 2021).

The duration of current flow is extremely brief, ranging from 0.06 milliseconds to 3 seconds. Pressure is maintained by the electrodes until the weld solidifies. Following this, the electrodes are opened, and the work piece is taken out. In RSW, copper electrodes,

classified into different classes (Class 1-3) to suit various materials, are brought into pressure contact with opposing faces of two superimposed metal sheets. The application of an electric current, be it AC or DC, occurs between these electrodes through the two metal sheets, leading to the formation of a weld joint.

Electrode materials, defined by ISO 5182 standards, mainly consist of copper alloys together with other alloying elements aimed at enhancing hardness without compromising electrical conductivity. Numerous research endeavors in the field of RSW have collectively identified crucial parameters that must be properly controlled to achieve an efficient and effective joint. These essential parameters include the current used, the time it takes the joint to form, the force used to hold the workpieces together, the thickness of sheet metal, the material used, and form of electrode.

The impact of conditions used for welding on the formed joints of magnesium alloy had been studied. As the time allowed for the weld to form increased, there was a corresponding enlargement of the size of the weld, together with a coarser microstructure of the nugget. A joint strength within the range of 2.9 kN to 3.05 kN was achieved when the weld time exceeded 6 cycles. Elevating welding current from 15 to 23 kA led to a rise in joint strength, attributable to the expansion of the nugget diameter, (Mashhuriazar, Mirsalehi, & Moradi, 2024). Their investigations have revealed that altering one or more of these parameters can significantly impact the microstructure of the weld and the resulting nugget diameter, ultimately influencing the strength of the joint. Various studies were conducted to establish the effects of welding parameters on the size of the nugget, (Azzouzi, Benkhedda, & Boumeddane, 2019).

Building upon this foundation, different researchers have conducted studies on the characterization of RSW, specifically employing an innovative annular recess electrode, (Watmon, Wandera, & Apora, 2020). Their studies revealed that this electrode exhibited superior strength and yielded a larger size of the joint compared to the solid electrodes.

This note- worthy finding has prompted further investigations, aiming to develop a design that would maximize the performance and give a more reliable spot weld joint. The pursuit of such insights is necessary for advancing the understanding of RSW and enhancing the effectiveness of metal joining techniques in practical applications.

1.2 Motivation for the Study

The manufacturing industry is so dynamic that it requires constant innovative ideas to reduce on material wastage, manufacturing costs and environmental degradation. At the same time, new materials have been designed and introduced in the automotive sector to enhance energy efficiency, reduce weight, ensure optimal speed. All these are intended to satisfy user requirements, and contribute to environmental conservation. These materials have been designed in varying gauges, diverse alloys, and composite structures, all calling for more research in support services including resistance welding processes.

More research in these services have explored the potential of an annular recess electrode design, (Watmon et al., 2020), (Ren, Zhao, Zhao, Liu, & He, 2019). The findings revealed promising outcomes, indicating an improvement in the spot weld characteristics. Building upon these findings, the motivation for this study hinges on the desire to design of an annular recess electrode that would give optimal performance and at the same time investigate the optimum parameters to be used to give a reliable spot weld joint. By

refining and fine-tuning the resistance spot welding parameters specific to the annular recess electrode, (Khuenkaew & Kanlayasiri, 2018b), this research is intended to support the evolution of welding techniques, aligning with the demands of modern manufacturing and automotive industries. The goal is to unlock the full potential of this innovative electrode design for improved weld quality and performance, addressing the evolving needs of materials used in these industries.

1.3 Problem Statement.

The mechanical properties of a spot-welded joint have a bearing on its physical characteristics, more especially the size of the joint formed, which is governed by welding conditions used and these plays a key role in determining the joint's strength and ductility. Welding current, electrode force, and weld time stand out as the three primary spot-welding process parameters controllable during Resistance Spot Welding, (Hamzah, Barrak, Abdullah, & Hussein, 2024). The welding conditions used are important in determining the properties of the weld and its integrity.

Most spot-welding studies done using the conventional solid electrode have shown little improvement on the size of the joint despite efforts made to improve the design of the electrode. Any attempts to increase certain welding parameters within a given schedule were always dictated by sheet metal conditions, risking expulsion and consequent loss of weld strength and electrode shape. The innovative idea of an annular recess electrode indicated that the size of the joint could be improved compared to the solid electrode. Therefore, the core issue at hand is having a good design of a spot-welding electrode which can produce quality spot welds with optimum performance. Addressing this

problem is paramount for advancing the field of resistance spot welding.

1.4 Justification of the Study

This study is intricately aligned with Sustainable Development Goal 9 (SDG 9), which emphasizes the enhancement of scientific research and the upgrading of technological capabilities within industrial sectors worldwide, particularly in developing countries.

Moreover, the study resonates with Uganda's Vision 2040, where industrialization is recognized as a pivotal growth opportunity to transition from a peasant community to a prosperous nation. To achieve this vision, Uganda aims to build a robust and competitive industrial base, crucial for job creation, technological advancement, and a resilient economy. The study supports Vision 2040's emphasis on developing local industries that harness local potential, specifically benefiting local car manufacturing industries like Kiira Motors. In line with the National Development Plan, (NDPIII) 2020/21 – 2024/25), which focuses on sustainable industrialization for inclusive growth, employment, and wealth creation, this study will contribute to establishing the automotive industrial, and Technology Park. This initiative supports various investments in the motor vehicle parts manufacture, vehicle testing, and automotive technology innovation. The study further addresses a key obstacle hindering the growth of Uganda's indigenous automotive industry, the low and isolated automotive value-added investment operating mainly as an informal sector. By establishing a connection between industry and academia, this research aims to strengthen efforts made by the informal sector engaged in building vehicles bodies, and parts, integrating much-needed engineering input for a robust automotive sector.

Furthermore, the study responds to the evolving landscape of the automobile industry, characterized by the emergence of new materials and metal alloys to address structural, environmental, and cost-saving concerns in car body manufacturing. These innovative materials necessitate advanced spot welding technologies, and the study extends existing knowledge on the application of annular recess electrodes in RSW through optimization of process parameters.

By doing so, this research not only supports the automotive industry's technological advancement but also contributes to the broader goals of sustainable industrialization, economic development, and inclusive growth in Uganda.

1.5 Research Objectives

1.5.1 Main Objective

The main objective of this study is to design an annular electrode with a recess that would give optimal weld quality and performance.

1.5.2 Specific Objectives

The specific objectives are:

(i) To establish the effect of process parameters on the nugget diameter of resistance spot welds made using a designed annular recess

(ii) To examine the effect of the process parameters on the strength of resistance spot welds produced using a designed annular recess

(iii) To establish the optimal process parameters for enhanced strength of resistance spot welds made using a designed annular recess

1.5.3 Research Questions

The research questions in this study are:

(i) How do welding current, welding time and electrode force affect the nugget diameter of resistance spot welds produced using an annular recess electrode?

(ii) How do welding current, welding time, and electrode force affect the weld strength of resistance spot welds produced using an annular recess electrode?

(iii) What are the optimal process parameter levels that result in the attainment of high integrity resistance spot welds?

1.6 Significance of the Study

The study relates to the optimization of performance of the novel electrode which is envisaged to find application in the automotive industry, among other application areas. As the developments in the automobile industry tend towards lightweight and high energy efficiency vehicles, there are equally developments in the materials to achieve the desired outcomes in the automobile industry. This study which develops an understanding of the optimal conditions of RSW of steel using an annular recess electrode will contribute to improving the integrity of the welds and the overall quality of the welded products produced by this type of electrode.

Optimizing the RSW undertaken in this study will improve the reliability of the welds through improved strengths leading to reduced cost of automobile body fabrication.

1.7 Scope of Work

This study involves a comprehensive investigation into the effect of three parameters namely, current, force, and time on the diameter, and strength of spot welds formed using

an annular recess electrode. The research questions guiding this exploration include inquiries into how current, time, and electrode force impact the diameter, and strength of spot welds formed with this electrode design. Additionally, the study seeks to determine the optimal levels of parameters that lead to the production of high-integrity resistance spot welds. The assessment of weld quality encompasses both destructive and non-destructive tests, aiming to ascertain the optimal values of these parameters for enhanced performance, characterized by increased nugget diameter, improved microstructure, and enhanced weld strength in resistance spot welds utilizing the annular recess electrode.

1.8 Conceptual Framework

This study establishes the effect of independent variables (welding current, welding time and electrode force) on the characteristics of the weld joint, namely nugget diameter, and weld strength (dependent variables). The conceptual framework is illustrated in the Figure 1.2 below.

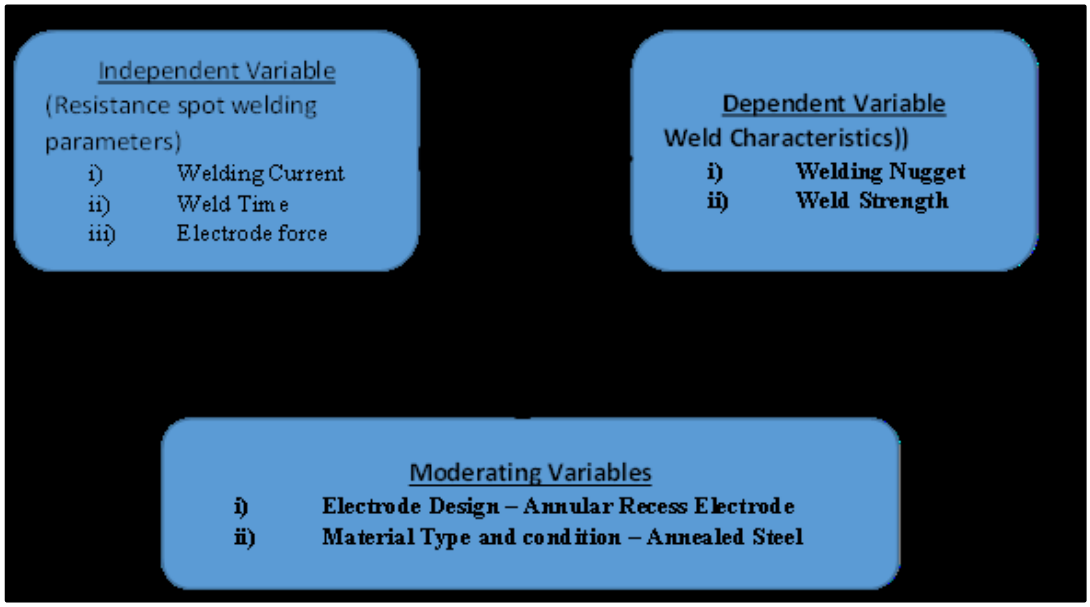

Figure 1.2: Conceptual framework for the performance of an annular recess electrode

CHAPTER TWO: LITERATURE REVIEW

This chapter presents a literature review on resistance spot welding which is helpful in setting a purposeful base for the study on the performance optimization of the annular recess welding electrode.

2.1 Principle of Operation of Resistance Spot Welding.

In principle, two workpieces are put in the machine between two copper electrodes which can be interchanged for different applications. During the joining process, melting of the two metals takes place on the contact surface due to the heat generated by the resistance to the flow of an electric current (I), (Alcantar-Mondrago´n, Reyes-Caldero´n, Garc´ıa-Garc´ıa, Garnica-Gonza´lez, & Estrada-Herna´ndez, 2023). As seen in the Figure 2.1 below, contact between the surfaces occurs when a force (F) is applied during and after the flow of the current, which in turn produces the forging of the weld metal. The process is completed within a specific time cycle. During Resistance Spot Welding, pressure is applied to hold firmly the workpieces together, (Tanmoy, 2022). The proposed voltage is then automatically switched on to ensure melting occurs at the interface.

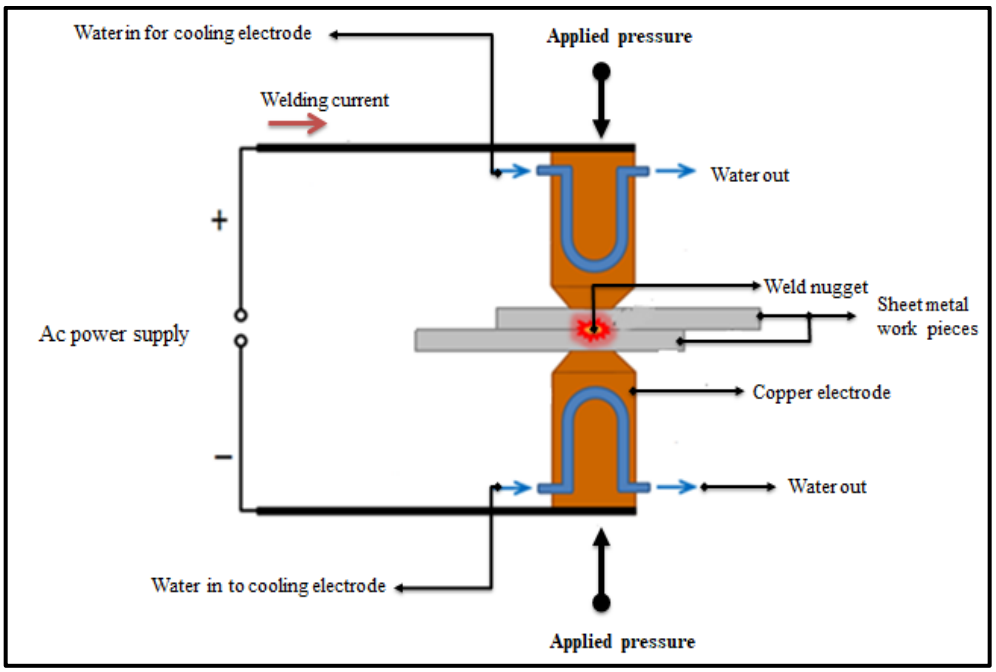

Figure 2.1: The spot-welding technique, (Watmon et al., 2020)

The proposed current and voltage of 5000A and 4-25V, respectively, supplied from the transformer through a short distance are required to localize the heating and produce the required amount of weld heating. The proposed current flow time is short between 0.06 milliseconds and 3 seconds. The electrodes maintain force until the weld solidifies. The work is removed by opening the electrodes. The RSW process is extensively applied to join a variety of sheet metal into complicated shapes with high accuracy and greater precision compared to other types of welding. It is mostly used in the automobile industry and its level of importance can be judged by the fact that in the car bodies there are between 3000 to 6000 spot welds. RSW can be used to join various metals alloys including ferrous and non-ferrous alloys. Studies have established that this method of spot welding can be used to join both similar and dissimilar metals to form a strong joint.

2.2 Effects of RSW Parameters

Spot welding involves complex interplay of factors that directly influence the weld quality. These factors are interconnected and minor adjustment in one parameter can impact on others. Achieving robust joints and high-quality welds hinges on the optimal selection and combination of these factors. Specific welding parameters play a crucial role in determining spot weld quality. Precise control of these parameters is essential for attaining the desired strength and quality of the joint. Optimization of the parameters is a key factor in achieving high-quality welds without incurring unnecessary costs while also improving throughput and efficiency. Various studies, such as those focused on shear strength optimization in stainless steel, highlight the importance of parameter control. Additionally, research exploring the use of different materials (316 austenitic and 425 ferritic stainless steel) aims to identify optimal conditions for conducting resistance spot welding, (Khuenkaew & Kanlayasiri, 2018a).

These studies collectively contribute to the ongoing efforts to establish robust and reliable spot- welded joints tailored to specific requirements.

2.2.1 Welding Current

During RSW, heat produced is directly proportional to welding current. Conventional RSW processes offer two types of waveforms i.e. Alternating Current (AC) and Direct Current (DC). In the automotive industry, single-phase AC spot welding is the predominant method. DC systems can be employed by converting single-phase or multi-phase AC into DC. Spot welders equipped with inverters can deliver high-frequency DC (up to 2000 Hz) enhancing energy efficiency. While DC-based spot welding typically

requires additional equipment leading to reliability issues and higher costs it minimizes heat loss and ensures a uniform heat flow. Welding current stands out as the most crucial parameter governing the heating of the workpiece that ultimately influences the development of the nugget. As welding current increases, there is a corresponding increase in root penetration and weld nugget diameter. However, if current is too low it fails to provide adequate heat for nugget formation. On the other hand, an excessively high current can result in welding defects. In the exploration of RSW parameters, it was observed that increasing welding current density enhances the shear strength but an excessive level can lead to defects and loss mechanical properties. Moreover, chosen current level has implications on the distortion of the base metal and the size of the heat-affected zone (HAZ), (Hassoni, Barrak, Ismail, & Hussein, 2022).

2.2.2 Welding Time

Weld time encompasses the duration required to complete a spot-welding process and includes three phases that are essential. These include squeeze, weld and hold time.

During welding, squeeze time allows welding current to delay until electrode force reaches the necessary level. Weld time refers to the duration when current flows into the metal before welding tales place. Hold time is that time allowed after welding is completed for the electrodes to remain in contact with the workpiece to cool the weld and allow the nugget to solidify. Providing sufficient weld time contributes to the formation of an appropriately sized and high-quality weld nugget, (Mashhuriazar et al., 2024). More so the importance of weld time in the context of RSW and the techniques for optimizing the process parameters is emphasized, (Kustron´, Korzeniowski, Piwowarczyk, & Soko-

lowski, 2021). It is crucial to note that increasing weld time without adequate welding current does not yield a satisfactory joint. Conversely, when welding current increases, the size of the nugget increases with longer weld time. However, an excessive increase in weld time can lead to workpiece expulsion. Hold time refers to the duration following the completion of welding for the electrodes to remain in contact with the workpiece. It helps to cool the weld while maintaining pressure after the weld has been completed. It is crucial that the weld nugget solidify before releasing the sheets. Figure illustrates the typical welding sequence. However, the duration of hold time must be carefully balanced as too much of it can result in heat from the point of welding spreading to the electrode resulting in its wear. Additionally, if hold time is prolonged and the material has a high carbon content (exceeding 0.1% carbon), there is a possibility of the weld becoming brittle.

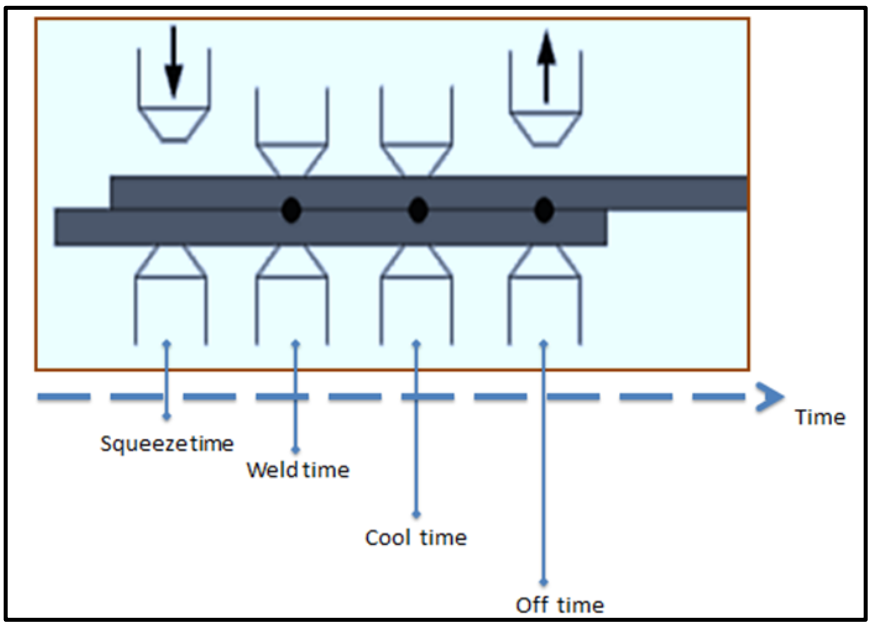

Figure 2.2: Typical welding sequence, (Matsukage, Sakurai, Traui, & Iyota, 2023)

There was a study conducted on the impact of weld time on nugget diameter for both the solid and annular recess electrode designs. The findings revealed that extending weld time

resulted in a larger weld nugget consistent with the findings of other researchers, (Ren et al., 2019), (Hassan & Lafta, 2023)

2.2.3 Electrode Force

Electrode force is that force exerted by the electrodes on the workpiece during spot welding. It significantly impacts on the resistance between electrode to metal and metal to metal contact. The magnitude of this force contributes to the occurrence of expulsion and formation of internal defects in the spot welds. Various studies conducted relating with electrode force revealed that this force is employed to ensure that current is distributed uniformly into the joint, (Taufiqurrahman et al., 2021). Electrode force directly affects resistivity of the circuit leading to variations in the quantity generated heat ultimately influencing nugget formation.

During spot welding, electrode force follows a distinct pattern including initiation, elevation to a specified value, stabilization during welding, a post-weld holding period and eventual release. This electrode variation is shown in Figure 2.3. These variations have an effect on the quality of the weld. The major role of this force is maintaining contact between the welded parts at the joint ensuring that there is continuous flow of electric current and ensuring that the necessary contact resistance is available at the point of welding.

The magnitude of this force is a critical variable that affects the welding outcome. If this force is excessively high, it reduces resistance to the flow of electric current from the electrode through the metal resulting in inadequate heat and insufficient melting of the material. This can also lead to undesirable heat conduction away from the weld area,

hindering nugget formation. Conversely, if it is too low it may lead to excessive heat generation causing distortions in the weld. In simpler terms, a low electrode force raises the likelihood of expulsion, (Xia, Su, Li, Zhou, & Shen, 2019).

Electrode force is important because it controls resistance between the electrode to metal and at the metal-to-metal interface which in turn affects heat generation, (Wohner, Mitzschke, & Juttner, 2020).

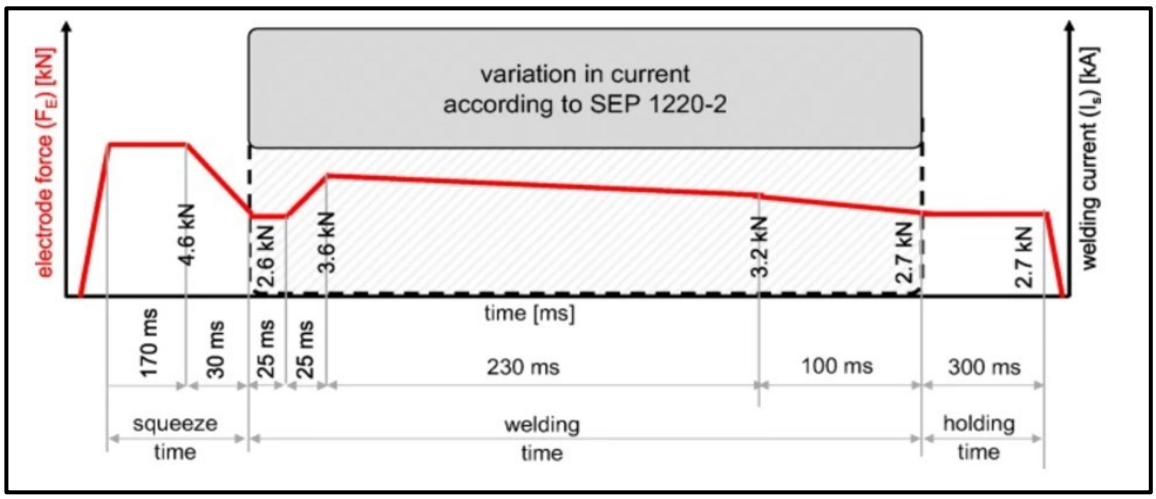

Figure 2.3: A schematic illustration of electrode force variation during spot welding.(Wohner, Mitzschke, & Juttner, 2020).

During the squeeze cycle, electrode force brings the sheet metal workpieces into contact and this influences contact resistance between the sheets. Therefore, increasing electrode force reduces contact resistance, which in turn increases current density and heat generation. This will lead to an increase in heat generation and melting rate of the material during spot welding for a given welding current and weld time. Studies by (Vishwakarma, Shrivastava, & Singh, 2018) and (Gawai & Sedani, 2019), using Taguchi method to optimize welding parameters on low carbon steel, indicate that electrode force is the most influential factor for controlling tensile shear strength. While investigating the welding of

dissimilar metals, AISI 304 and 1060, it was observed that the strength of the joint for dissimilar metals decreased with increasing electrode force, (Yang et al., 2024). This decrease in joint strength was caused by the increase in electrode force which led to a decrease in electrical resistance accompanied by a reduction of heat energy in the welding area.

During the study on the impact of electrode force on RSW, it was observed that an excessively large electrode force led to expulsion, (Yang et al., 2024).

This happened because the molten pool extended beyond the area confined by the electrode force. Conversely, too small an electrode force may result in expulsion due to instability between the electrode and the work piece contact, significantly compromising weld strength and electrode integrity. In a study conducted on the relationship between electrode force and weld nugget size it was observed that increasing the electrode force led to a decrease in nugget size, (Khader, Valappil, Murad, & Abu Qudeiri, 2023). This was attributed to the increase in contact surface area of the faying surfaces with increased electrode force. As resistance is inversely proportional to contact area, the higher the contact area the lower the resistance and consequently the lower the heat generation resulting in a smaller nugget size. This finding aligns with the conclusions drawn by other researches utilizing the finite element method to study nugget size in the RSW process, (Perulli, 2020). Although increase in electrode force is associated with decrease in contact resistance, a higher electrode force is necessary for the formation of a robust nugget. Importantly, a higher electrode force helps prevent the occurrence of expulsion providing a significant advantage in the welding process.

2.2.4 Electrode Geometry and Design

In RSW, welding current is permitted into the workpiece through the electrode. Therefore, it is logical that the electrode's geometry controls specific weld characteristics. Since the shape and size of the welding electrode impacts on the outcome of the weld, the weld nugget should be smaller than the electrode diameter. The form of welding electrode important because it determines the welding process and properties of the weld. Studies have shown that the shape and form controls current density, which is responsible for the formation of weld nugget, (Reddy Gillela, 2023).

These factors further affect focalization of force, current density of the weld interface and weld area's location. Further studies conducted on the qualities of electrodes led to the conclusion that the geometry of electrode tips can also influence how well the weld nugget can form, (Khuenkaew & Kanlayasiri, 2018). Other studies on electrode geometry revealed that the size and shape of the welds formed are influenced by the size and formation of the electrode, (Chen, Wang, Wang, Carlson, & Sigler, 2019).

Studies further revealed that during RSW, the current that spreads into the workpiece during RSW enters near the electrode edge causing current constriction at that point, this leads to uneven heating across the electrode face which promotes localized wear, (Abass, 2023). He further observed that electrode geometries that exhibit large current densities near the outer face edge exhibit different welding characteristics than those with uniform current distribution. This is because the former would leave less current available for nugget formation at the faying surface beneath the electrode. The failure load of a joint is determined by the size of the nugget and effective control of heat distribution at the faying

surfaces of the workpiece is essential in influencing the nugget size. Researchers have conducted studies, particularly focusing on annular recess electrodes to understand the heat distribution around the electrode and alter the nugget growth mode.

In a specific study involving a ceramic- filled annular recess electrode designed to regulate heat distribution in the welding process, the energy is dispersed in the annular conductive region rather than being concentrated in the center of the nugget. The findings suggest that with this annular design, the nugget grows both inward and outward from the initial ring formation, resulting in a larger nugget area.

This innovative approach to heat distribution control in welding electrodes showcases potential benefits in achieving specific nugget growth patterns and influencing overall joint strength. Studies on electrode geometry in RSW have become an intriguing area of research. The shape of an electrode influences the final shape of the weld nugget.

The area around the electrode face determines current density, the rate of cooling and their combined effects on the weld nugget and electrode deformation, (Liu, Wei, Wu, & Zhang, 2020). Figure 2.4 shows the different types of electrode design, (Abass, 2023). In a separate study on examining the effects of electrode geometry on current distribution around the electrode face, it was observed that during the resistance welding, current diverges into the work piece. Because there is substantial concentration of current near the outer edge of the electrode face, this can result in less current being available for nugget formation at the faying interface directly beneath the electrodes.

The geometry and dimensions of both the electrode and work piece have a notable impact on the distribution of current density, ultimately influencing the size of the weld nugget, (Kimchi & Phillips, 2023). If the electrode tip diameter is small for the application, it can lead to a weld nugget that is undersized and weak.

Conversely, if the diameter is large there will be a risk of overheating the base metal which potentially causes the development of voids and gas pockets. In essence, achieving an optimal balance in electrode geometry is crucial for ensuring the strength and quality of the weld.

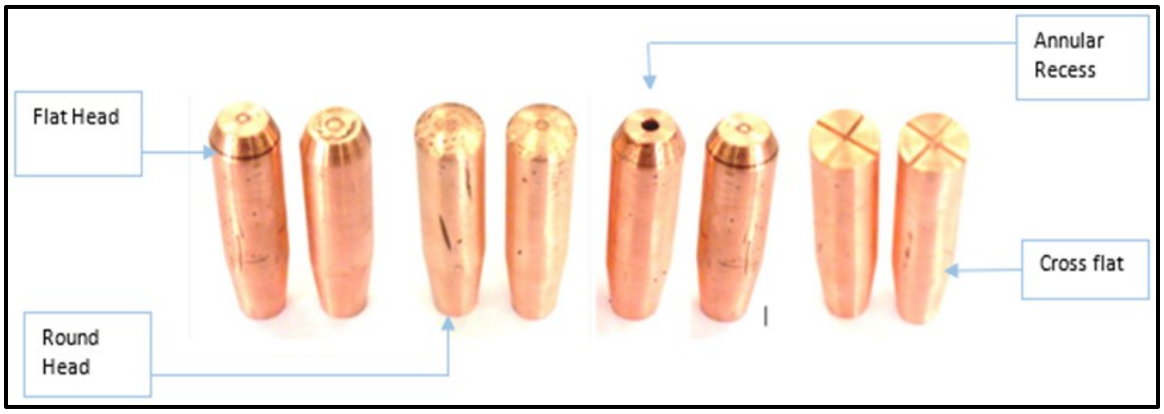

Figure 2.4: Illustration of the different types of electrode geometries

(Abass, 2023) Research on the designs of electrodes in RSW has revealed that the geometry of an electrode has a big bearing on the way current flow through it and the way it is distributed to the work piece which eventually determines its life. Studies have demonstrated that electrode bigger-worksheet interface angles contribute to a more uniform current distribution at the electrode face. This effect reduces localized heating at the face periphery potentially leading to more un even wear and rapid mushrooming of the tips.

In a study on the impact of process parameters in RSW, it was found that metals with different thicknesses require varying parameter settings, (Mumtaz, 2020). A general criterion in RSW is to achieve a nugget diameter of ($5\times t$ (1/2)) where" t" represents the thickness of the metal sheet. It is crucial to maintain electrode life for acceptable welds, (Liu et al., 2020). Avoiding electrode degradation is essential because it can lead to defects in the weld nugget. During electrode degradation, the contact area of the electrode increases to a size with in- adequate current densities resulting in poor weld quality. In the domain of RSW electrode geometry, it is important to consider a design which balances both mechanical and thermal properties while ensuring uniform current distribution. This underscores the need to optimize electrode design for longevity and consistent welding performance.

Different researches focusing on electrode tip selection for RSW of dissimilar stainless steels aiming at identifying the most suitable electrode tip in terms of weldment quality characteristics such as penetration, indentation depth and nugget diameter have been made. Various electrode tips with different geometries all made from the same material and thicknesses were used in the study.

The key conclusion drawn from the research emphasizes the importance of tailoring electrode design to the specific welding task at hand. This is because the nature of the electrode design and its morphology significantly influences nugget formation. In essence, the study underscores the need for a thoughtful selection of electrode design that would favour certain requirements for process optimization to achieve a quality weld. A comparative study on the performance of RSW electrodes specifically examining an

annular recess versus a solid electrode in welding a 1mm steel sheet grade used in automobile structural body was con- ducted with an objective of investigating the effects of welding parameters on weld strength for both electrode designs. This study concluded that the former outperformed the latter in terms of tensile strength and size of nugget diameter. Figure 2.5 below shows the design of an annular recess electrode, (Ren et al., 2019).

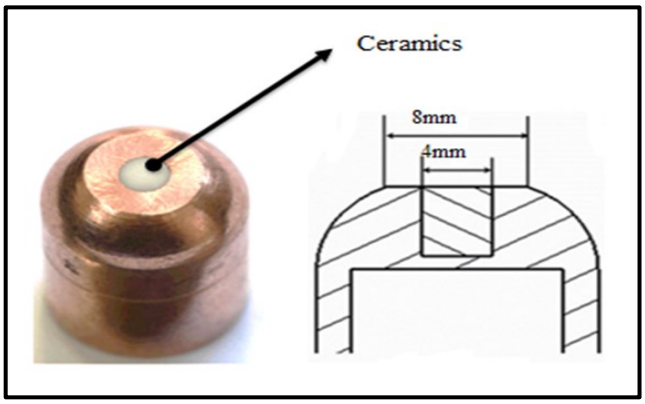

Figure 2.5: An illustration of the design of an annular recess electrode (Ren et al., 2019b)

2.3 Weld Nugget Growth

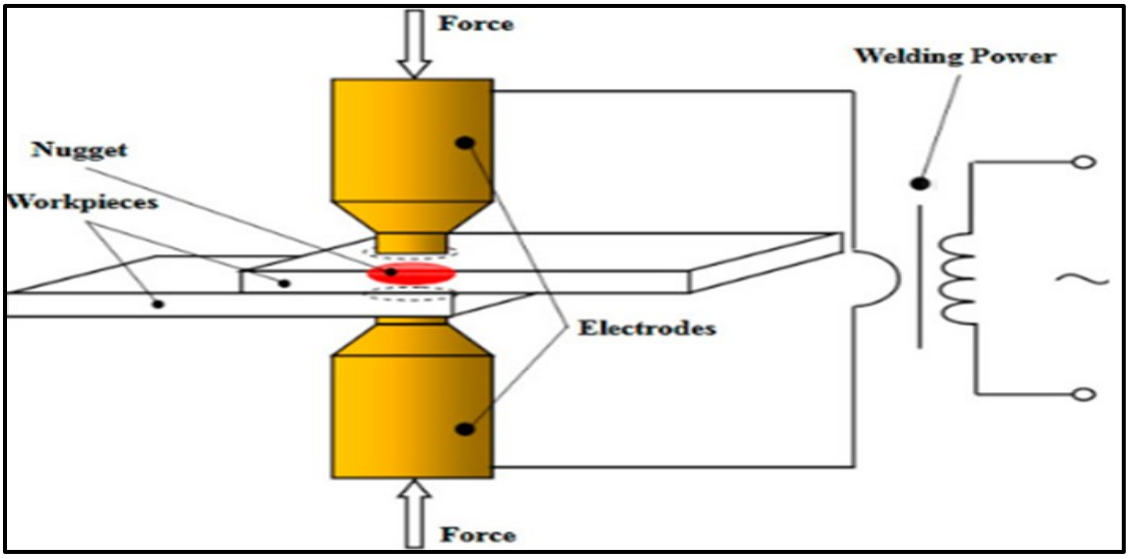

Figure 2.6: A diagram illustrating the formation of weld nugget (Luo et al., 2016)

The weld nugget is a pivotal element in RSW that determines the strength of the joint. Its growth hinges on key factors such as welding current density, the duration of current delivery, pressing electrode force and the available area for current delivery. Higher current densities contribute to increased heat generation while sufficient time for current delivery, appropriate electrode force and effective current distribution across the available area collectively influence the size and characteristics of the joint, (Qiu, Li, Shi, & Yu, 2023). This interplay of factors is critical as it determines the overall quality of a welded joint highlighting the importance of carefully controlling parameters for optimal weld nugget formation and consequently joint integrity. (Azzouzi et al., 2019), have demonstrated that the nugget size is crucial in determining the failure load of a joint with a larger nugget providing a more substantial safety factor. Figure 2.6 above shows an illustration of how a weld nugget is formed.

Ensuring the strength of joints especially in high-strength steel welding processes, necessitates achieving a robust nugget and providing for a wider coverage of parameters from which to choose the best for optimal performance. The approach to obtaining larger nuggets in RSW involves increasing the size of the electrode tip together with the welding parameters. Excess current can quickly cause spattering introducing internal defects in the nugget. In optimizing the welding parameters, a careful balance must be struck to achieve large nuggets without compromising the overall integrity of the joint.

In a study to explore the relationship between electrode force and nugget growth with regard to metal contact resistance, it was found out that lighter electrode forces contribute to higher contact resistance. This is caused by the smaller percentage of the contact area

engaged resulting in a reduction in nugget size. In essence, the relationship suggests that as the electrode force decreases the contact resistance increases ultimately impacting the size of the weld nugget emphasizing the intricate balance needed in optimizing electrode force for effective Resistance Spot Welding (RSW), (Hoseini et al., 2017). Conversely, as the electrode force increases contact resistance reduces by expanding the contact area but this also decreases the nugget size. Another notable observation from the same study was that the thickness of the plate influences the weld nugget's size. An increase in plate thickness leads to radial growth but axial reduction in the weld nugget due to heat loss in the radial direction. In a separate experimental study on RSW of austenitic stainless steels, increasing welding current had more impact on nugget growth than it had on increasing weld time. Prolonged weld time with a constant welding current resulted in increased heat loss and reducing the nugget growth. The researchers also observed that extending weld time without a concurrent increase in welding current shows no significant sensitivity to expulsion, (Xia et al., 2019).

In the study investigating the connection between electrode force and nugget growth in the context of faying contact resistance, it was observed that lighter electrode forces led to higher contact resistance due to a smaller percentage of the contact area being engaged. This in turn resulted in a reduction in nugget size. Simply put, decreasing the electrode force was associated with increased contact resistance and a subsequent decrease in the weld nugget. (Azzouzi et al., 2019). Figure 2.7 above illustrates this theory.

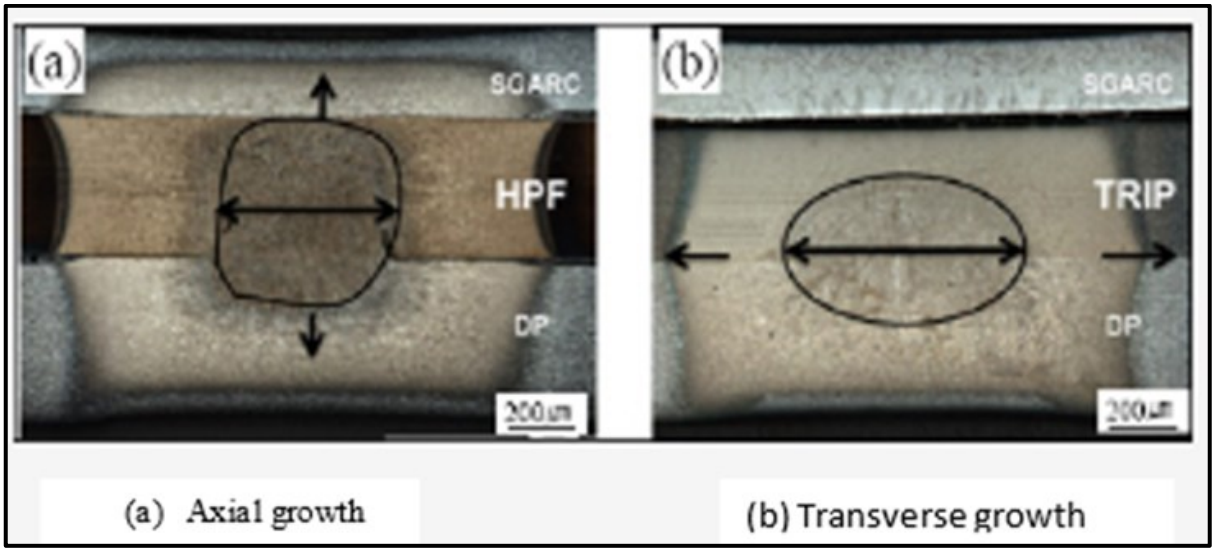

Figure 2.7: Shows the effect of electrode force on nugget growth, (Huda et al., 2019)

2.4 Quality Control in RSW

Assessing the quality of RSW can be challenging as appearances can be deceptive leading to the possibility of a seemingly good weld lacking structural integrity. To address this, industry practices often employ quality tests, (Zhou & Yao, 2019). Various factors can affect spot weld quality, giving rise to defects that fall into two main categories. These are non-surface-breaking discontinuities and surface-breaking discontinuities. Non-surface breaking discontinuities encompass welds with little to no fusion, cold or stuck welds and variations in weld nugget size.

On the other hand, surface-breaking discontinuities include weld expulsion, indentation, and weld cracks. These classifications provide a framework for identifying and addressing the diverse array of defects that may compromise the quality of spot welds in industrial applications. Experimental results demonstrate the system's capability to identify spot welds gauge nugget diameter and leveraging this information differentiate between spot welds and stick welds. The system exhibits the capacity to inspect over four spot welds

per minute, showcasing its potential as an automated non- destructive spot weld inspection system, (Runnemalm et al., 2014).

Several defects can be experienced in metal manufacturing using RSW. These include in-complete fusion or lack of penetration, where inadequate welding current results in a weak joint, burn-through caused by excessive current leading to material burning and hole formation, overlapping or over burning, occurring when spot welds are too close or excessively heated, enlarging the weld nugget size, expulsion, involving molten metal expulsion and weakened welds. Other defects include cracking due to rapid cooling or high residual stress, undercutting, eroding base material along weld edges and reducing load-bearing capacity and electrode indentation, resulting from excessive force or misalignment, (Wang et al., 2016). Careful control of welding parameters along with regular monitoring, is essential to minimize these defects and ensure high-quality welds, (Wan et al., 2014). Evaluation of resistance spot welded joints predominantly centers on the attained strength, a parameter significantly influenced by the formation of the weld nugget, (Ghatei-Kalashami et al., 2022). Quality control procedures for spot welds typically involve either destructive or non-destructive testing methods. Figure 2.8 show the destructive testing method using a peel test, (BWS, 2019).

In the case of destructive testing, the strength of individual spot welds is commonly assessed manually using methods such as peel or chisel testing. These approaches provide a means to gauge the integrity and strength of spot welds aiding in quality control efforts within industrial applications.

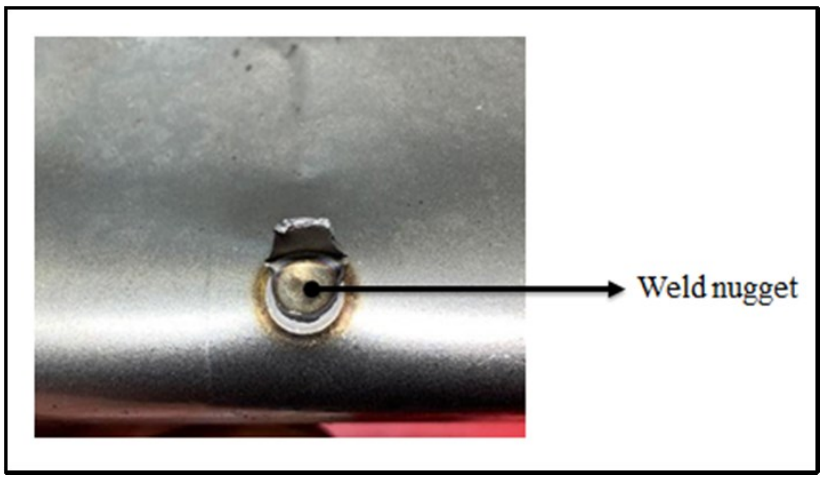

Figure 2.8: Second figure on destructive testing using peel test method (BWS, 2019).

Peel testing serves as a valuable method in welding quality assessment, providing a visual reference to ensure that the weld being produced aligns with the specified size, shape, and overall integrity. This testing process involves carefully peeling or separating the welded components, allowing for a detailed examination of the resulting joint. By visually inspecting the weld after the peel test, manufacturers can verify its conformity to the required standards and specifications.

2.5 Optimal Parameters of Spot Welding

The load-bearing capacity of a spot weld is determined by three main parameters namely; welding current, weld time and electrode force. Manufacturing engineers face the challenge of identifying the parameters for spot welding to produce welds with high tensile strengths and minimal internal defects at lower manufacturing costs.

This optimization process depends on factors such as material properties input process parameters and the welding process it- self, (SA Jadhav, 2016). The control and optimization of welding processes and parameters play a crucial role in directly

influencing product quality and performance, (Raut & Achwal, 2014). Despite current practices relying on welding schedules based on experience, hand- books, and welding tables the selected welding schedule does not guarantee optimum spot weld characteristics. Therefore, the identification of an optimum welding schedule becomes essential for creating joints with the desired weld characteristics. In RSW, the quality of a weld is defined by three dependent variables namely; shear strength, weld indentation, and diameter of nugget. The key parameters influencing RSW quality have already been discussed and variations of these parameters can lead to changes in the mentioned variables. For instance, increasing the welding current results in an increase in the diameter of the nugget, and tensile shear strength of the weld. Similarly, increasing the weld time while decreasing the electrode force will lead to an increase in weld nugget growth and tensile shear strength.

Tensile shear strength is the most critical and influential factor in optimizing welding parameters, (Raut & Achwal, 2014). An experiment was conducted with an objective of determining the significant levels of parameters for optimal tensile strength and nugget diameter, (Rawal et al., 2016). The objective of this study was to optimize welding parameters with tensile shear strength and nugget diameter as response variables. The researchers established that welding current was the most significant parameter among the three for both variables. The researchers concluded that these parameters are essential factors for determining the tensile strength of a joint and that a suitable combination of them is necessary for maximum strength, (Raut & Achwal, 2014).

They further observed that welding current was the main parameter that may affect the strength of the weld joint, (Halim, 2018). An experimental investigation was conducted to determine the optimal parameters of RSW for AISI 316L stainless steel using the Taguchi Method, (Vishwakarma et al., 2018). The primary goal was to enhance the tensile strength of the joint. The results revealed that the most significant parameters influencing tensile strength were electrode diameter, welding current and heating time contributing 66.09%, 25.08%, and 2.29%, respectively. Similarly, researchers focused on investigating the influence of parameters namely current, pressure, and welding cycle on the RSW of ASS316 material with specific emphasis on analyzing the resulting impact on hardness. The findings unequivocally indicated that these parameters exert a substantial influence on the variation in percentage improvement in hardness of ASS316 steel.

The study underscores the significance of considering and optimizing these parameters to achieve desired hardness outcomes in the context of RSW of ASS316 material, (Khuenkaew & Kanlayasiri, 2018b). Their study employed Analysis of Variance (ANOVA) and Signal-to-Noise (S/N) ratio to identify significant parameters and quantify their impact on response characteristics, (Yasin et al., 2020). The findings indicated that increasing the welding parameters led to an increase in the diameter of the nugget along with increased weld indentation. It was concluded from the research that increasing welding current and weld time makes the mode of failure of the spot welds to shift from interfacial to pull-out mode. This transition occurs because increasing welding current and time leads to formation of a larger nugget diameter, capable of resisting forces causing interfacial failure. Consequently, achieving a suitable combination of welding parameters, known as the welding schedule, is crucial.

This observation was affirmed by the investigation of the effect of welding parameters on tensile strength in the RSW, (Odiaka et al., 2021).

2.6 Gaps inKnowledge

In the study conducted by (Watmon et al., 2020), the anticipated linear relationship between electrode geometry and nugget diameter did not align with the actual results obtained. The analysis of variance revealed that variation in the strength of the weld and nugget diameter for the two types of electrodes was not significant. Additionally, the researchers observed that the analysis of variance on the effect of welding current on nugget diameter for both types of electrodes was not significant highlighting the potential presence of additional factors influencing these outcomes. While the researchers noted improvements in maximum tensile load and an increase in nugget diameter when using an electrode with an annular recess, the scope of study did not allow for the determination of optimal parameters. Consequently, this study aims to fill these gaps by determining the optimal RSW parameters for the specific electrode design and examining the overall integrity of the joint.

CHAPTER THREE: METHODOLOGY

This chapter presents the research methodology, the test materials, test equipment and tools used in the study, the experimental design and data analysis techniques.

3.1 Research Methodology.

Various studies on RSW of different materials and conditions indicated that the most significant parameters that require optimization to attain high-quality spot weld include: welding current, weld time, and electrode force. A welding schedule using an annular recess electrode was explored in this study to produce flawless resistance spot welds of high integrity defined by high strength. Therefore, this study was intended to come up with a design of an annular recess electrode and determine the optimal parameters by examining the joint integrity.

3.2 Research Design.

This experimental study was designed to help in determining the impact of RSW parameters on the quality of spot welds in mild steel, employing an annular recess electrode. The investigated parameters encompassed welding current, electrode force, and weld time. The study focused on key weld quality attributes namely; nugget diameter, and weld strength, as output variables. The research delved into examining the effects of each parameter on the specified output variables. To optimize the process for achieving maximum nugget diameter and weld strength, the Taguchi orthogonal array was employed as part of the research design, providing a systematic approach to parameter optimization. The research design is illustrated in Figure 3.1.

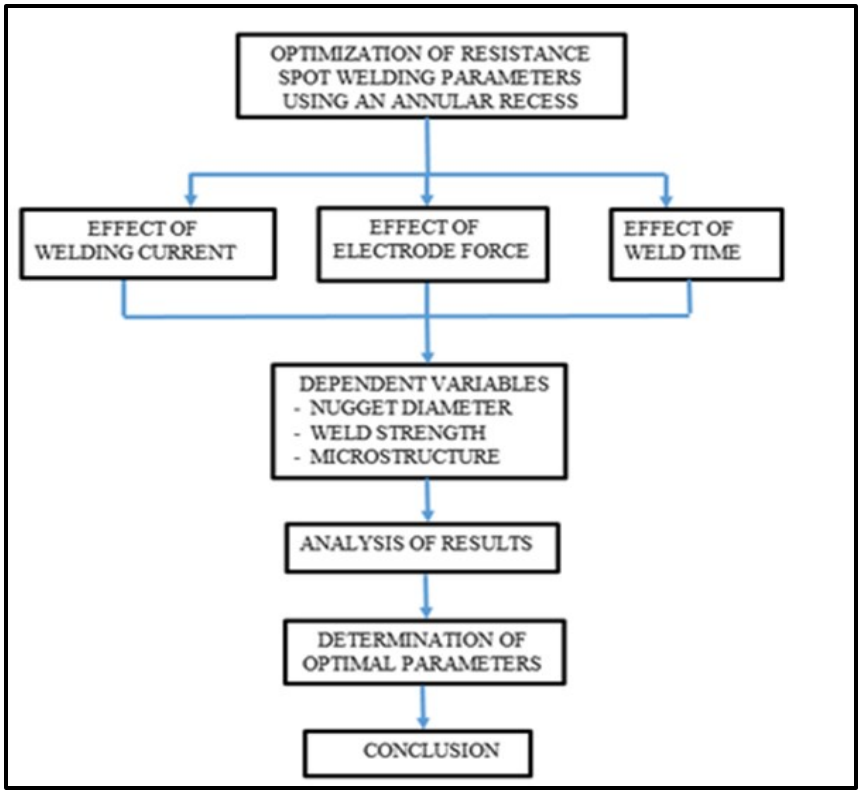

Figure 3.1: Illustration of research design

3.3 Description of Materials

3.3.1 Description of Sheet Metal Used.

The sheet metal utilized in this study was sourced from the bonnet of an older model of the Toyota Corolla, specifically the E-AE91-BEMEK model. To ensure optimal conditions for the spot welding process, the sheet metal underwent a meticulous cleaning process. Initially, a paint remover was applied to eliminate any surface paint material. Subsequently, the material underwent a thorough cleaning using sandpaper to eliminate any residual layers such as oxides or paint that could potentially interfere with the welding process and compromise the quality of the weld. The material with a thickness of 1mm was then precisely cut into strips measuring 100mm x 25mm using a shearing machine.

This careful preparation of the sheet metal aimed to create an ideal substrate for the subsequent spot welding experiments**.**

3.3.1.1 Mechanical Properties of the Sheet Metal Material Used.

The mechanical properties of the sheet metal under consideration encompassed hardness, tensile strength, elongation, and strength. These properties were precisely determined through testing conducted at the laboratory of the Roofing Rolling Mill factory located in Namanve, Uganda. The obtained mechanical property data serves as essential information for under- standing and characterizing the behavior and performance of the sheet metal material during the spot-welding experiments conducted in the course of this study.

3.3.2 Description of Electrode Used.

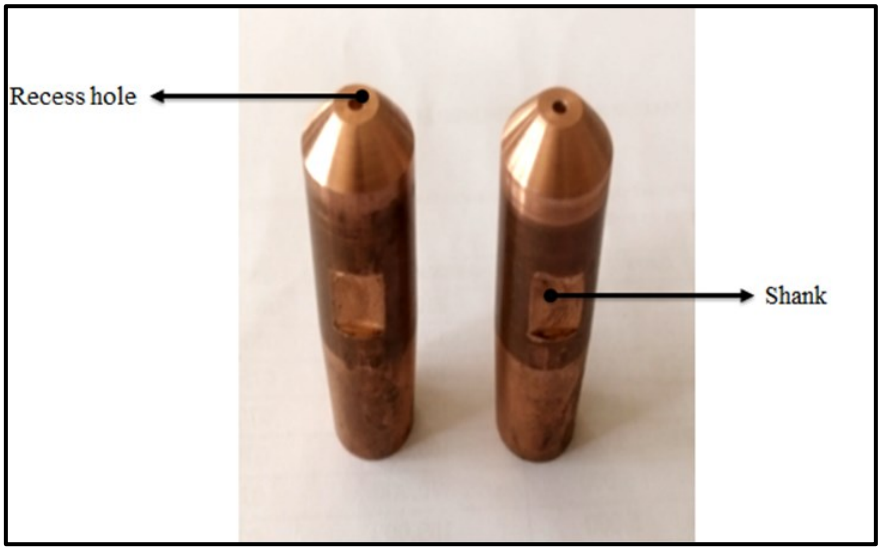

Figure 3.2: The samples of the machined electrodes.

In this study, an annular copper electrode was employed crafted from a copper rod of diameter 15mm. The rod underwent machining to achieve specific dimensions featuring a 45-degree conical end with a diameter of 8mm.

A central recess hole measuring 3mm in diameter and 6mm deep was machined in the electrode. Within this recess hole an insulating material specially prepared for the purpose was inserted. This electrode design was chosen to suit the resistance spot welding experiments conducted in the investigation ensuring precise and controlled conditions for the welding process. After prolonged usage of the electrode, a notable observation was made regarding the insulating material indicating a tendency for it to dislodge. As a remedy, the electrode underwent a modification wherein the previously smooth hole was threaded. This internal threading was intended to enhance the retention of the insulating material preventing it from falling out during the spot welding process. This modification proved essential in addressing the practical challenge encountered during the electrode use ensuring more stable and reliable performance over time. The samples of the machined electrodes are shown in Figure 3.2 above.

3.3.2.1 Properties of Copper Electrodes.

Table 3.1: Main properties of copper

Molecular weight	63.55
Appearance	Reddish metal
Melting point	1085°C
Boiling point	2562°C
Density	8.96 g/cm^3
Solubility in water	N/A
Electrical resistivity	1.673 μΩ-cm @ 20°C
Electronegativity	1.90 Paulings
Heat of fusion	13.26 kJ·mol^{-1}
Heat of vaporization	300.4 kJ·mol^{-1}
Poisson's ratio	0.34
Specific heat	0.39 kJ/kg K
Thermal conductivity	401 W·m-1·K-1
Thermal expansion	(25 °C) 16.5 μm·m^{-1}·K^{-1}
Vickers hardness	369 MPa
Young's modulus	110–128 GPa

Copper electrodes exhibit a distinctive set of properties that render them indispensable in various applications as seen in the Table 3.1 above. With a molecular weight of 63.55 and a reddish metallic appearance, copper has melting and boiling points of 1085 ^{0}C and 2562 ^{0}C respectively. Its density of 8.96 g/cm^3, along with notable electrical properties such as an electrical resistivity of 1.673 $\mu\Omega$-cm at 20 ^{0}C, makes it an excellent conductor. Additionally, copper demonstrates favorable mechanical characteristics, including a Vickers Hardness of 369 MPa and a Young's Modulus ranging from 110 to 128 GPa. These properties, coupled with its thermal conductivity, solubility, and specific heat, collectively contribute to the versatility and reliability of copper electrodes in various industrial and research settings.

3.3.3 Insulating Material

The insulating material employed in this study comprised a blend of clay, kaolin, and white cement. The preparation involved mixing white cement with kaolin in an approximate ratio of 1:1. Subsequently, this mixture was combined with well-prepared and thoroughly blended clay to ensure a homogeneous composition. The resulting mixture was then inserted into the recess hole of the electrode. This carefully crafted combination of materials aimed to provide effective insulation of the electrode, enhancing its performance during the spot-welding process.

3.4 Description of the EquipmentUsed

3.4.1 Equipment for Determining the Hardness of the Material

The apparatus employed for assessing the hardness of the material belonged to the Roofing group Limited and was a Rockwell Hardness Tester Model JMHR – 150 ZS

with the serial number JM031028. This equipment designed with a capacity of 100kg and utilizing the HRB scale helped in determining the hardness of the material under investigation. Figure 3.3 below shows the equipment used to determine the hardness of the material.

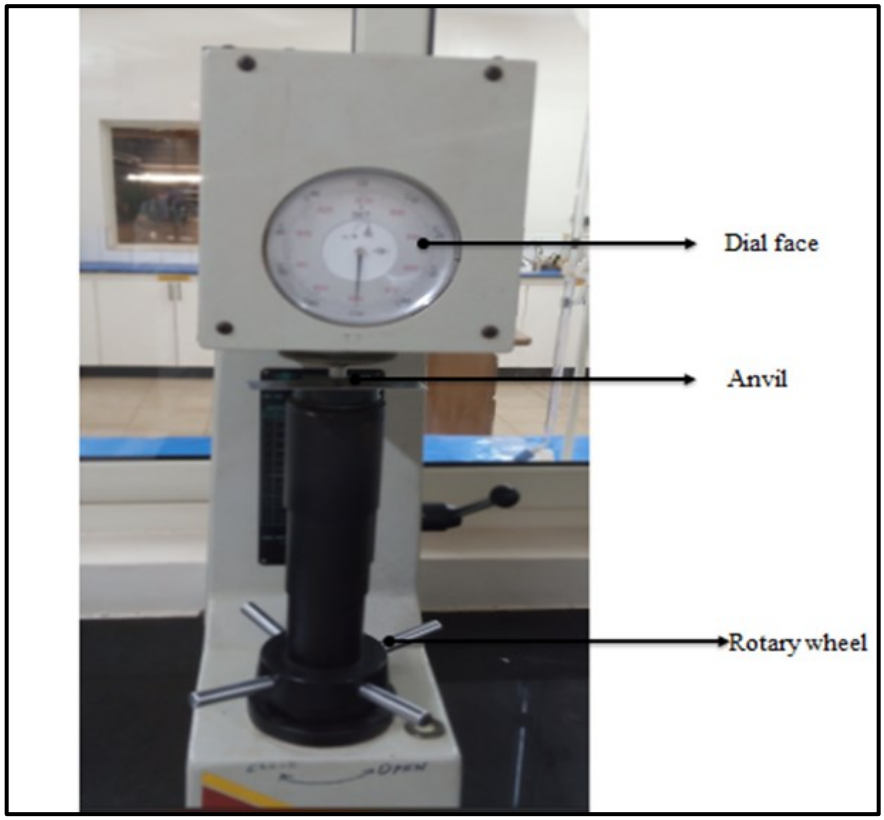

Figure 3.3: The specific Rockwell Hardness Tester used in this study (with permission from Roofings Rollings Ltd.)

3.4.2 Equipment for Determining the Strength and Elongation of the Material

The apparatus utilized to conduct strength tests on the spot welds was a tensile testing machine model UTN 7E-100, with the serial number 4/2010 -4320 and a capacity of 1 MN. This specific testing machine owned by Roofing Ltd in Kampala was used to determine the strength of the welds under investigation. Figure 3.4 below shows the equipment used to determine the strength and elongation of the material.

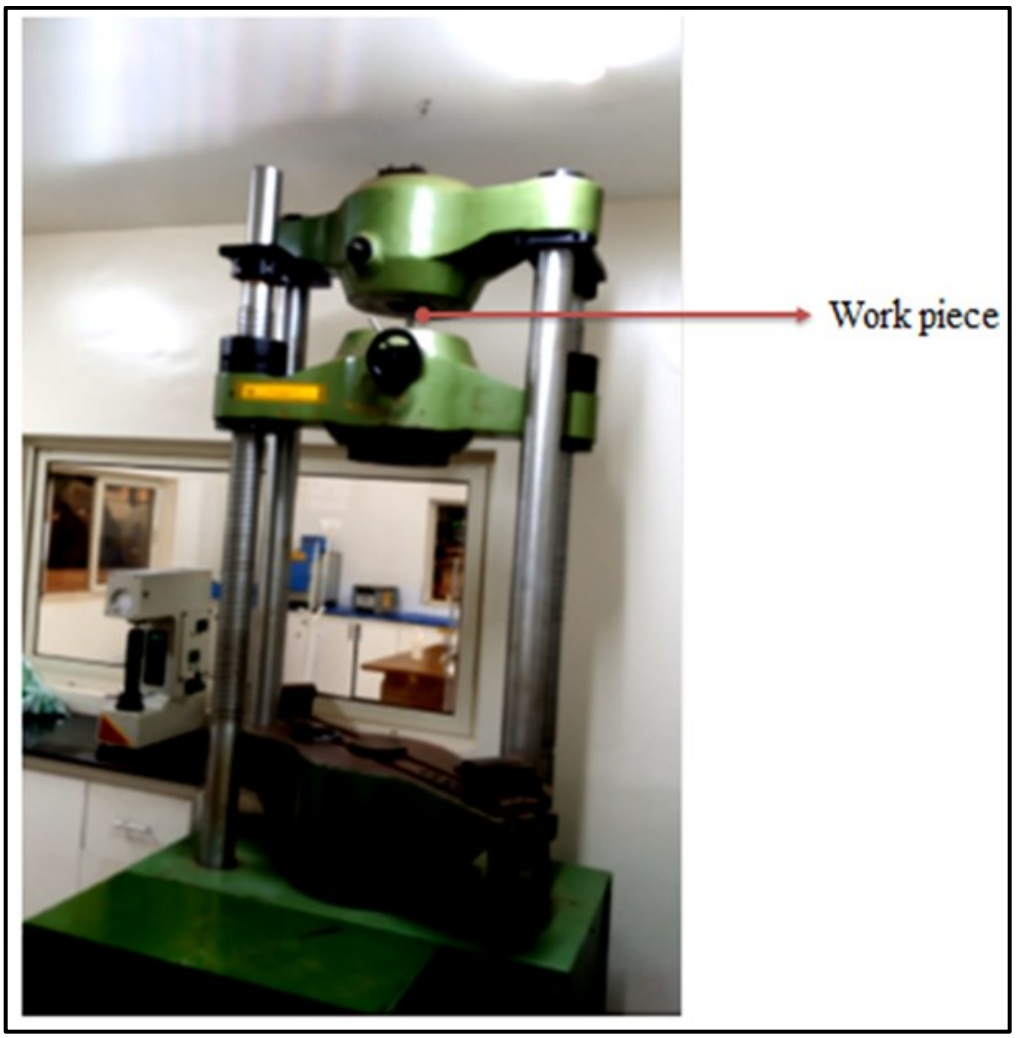

Figure 3.4: The tensile testing machine that was used in the study (with permission from Roofings Rollings Ltd.)

A total of two samples underwent testing to determine their tensile strength and elongation properties. The testing process involved obtaining individual values for tensile strength and elongation for each sample. Subsequently, the average values for both tensile strength and elongation were determined using the results of the two tested samples. This approach allowed for a more representative assessment of the material's mechanical properties.

3.4.3 Spot Welding Equipment Used: UTOSpot Welder (Model S1-6-354, Serial No. 21563)

The spot-welding process utilized the UTO Spot Welder, specifically the model S1-6-354, identified by Serial No. 21563. This equipment boasts a rated capacity of 35KVA, operates at a frequency of 50Hz, and requires a water supply of 6 liters per minute. Additionally, it exerts an electrode pressure of 255kgf during the welding process. Noteworthy features of the spot welder include a timer for precise adjustment of welding parameters and a pressure regulating valve facilitating the fine-tuning of electrode pressure. The machine used to conduct the experiment is indicated in Figure 3.5 while Figure 3.6 indicate the spot-welded samples.

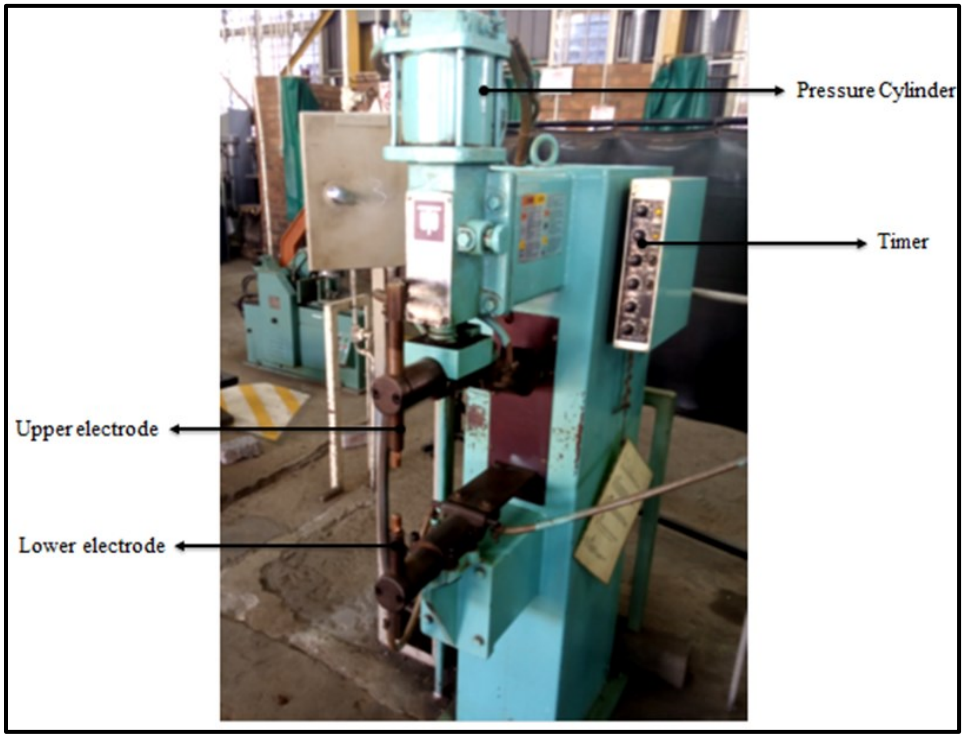

Figure 3.5: Spot welding machine used (with permission from Nakawa Vocational Training College)

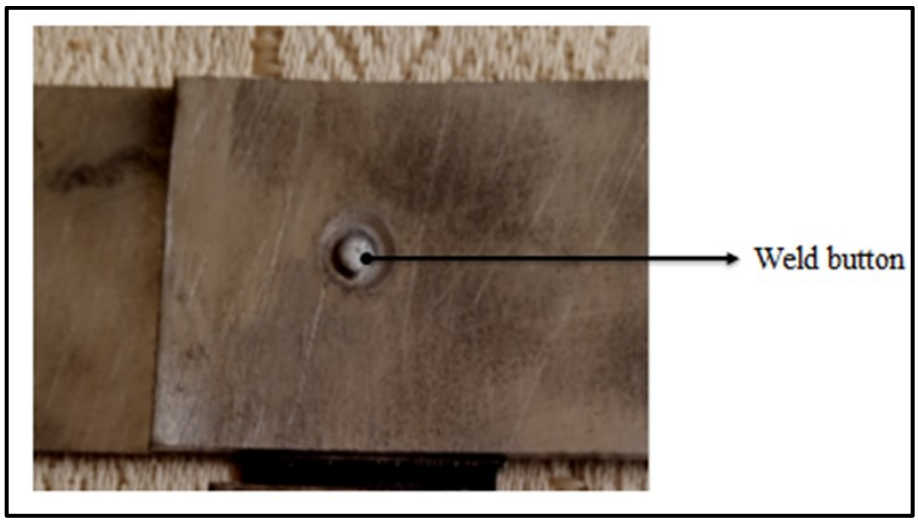

Figure 3.6: Sample of spot welded workpiece used in this study

The choice of a specific parameter is determined by the number of levels for various factors. In experimental studies, a Taguchi orthogonal array was employed for three process parameters, each having three levels. The images shown in Figure 3.7 below display the spot-welded specimen based on this array. Each experiment is repeated three times to establish the impact of parameters at various levels on performance characteristics

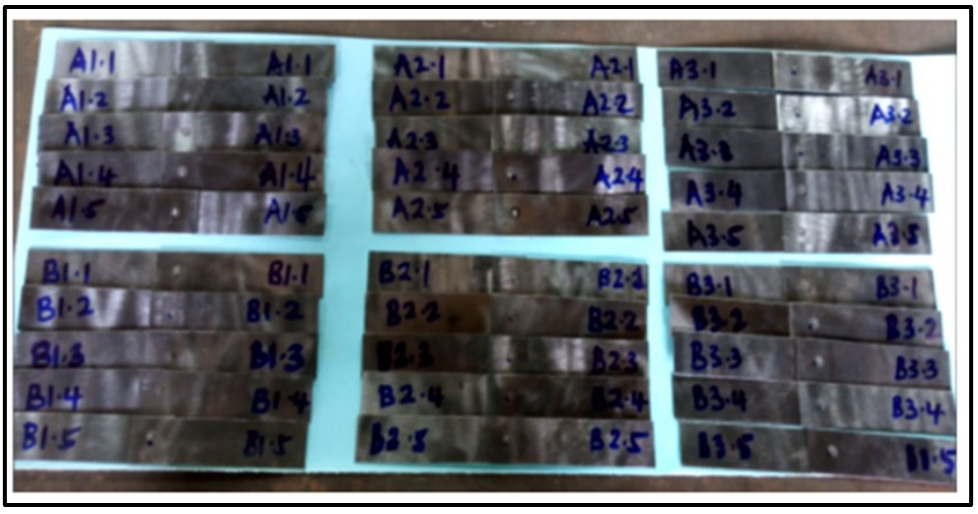

Figure 3.7: Picture showing sets of spot-welded specimen

3.4.4 Equipment for Determining the Material Composition

The assessment of sheet metal composition was conducted using a mass spectrometer machine sourced from the Roofing Group. This specialized equipment was used to determine the elemental composition of the material under investigation. The mass spectrometer's capability to analyze the material at the molecular level provided crucial insights into the com- position, aiding in the comprehensive understanding of the sheet metal's chemical makeup and contributing valuable data for the research study. Figure 3.8 below shows the equipment used to determine the material composition while the Figure 3.9 illustrates the testing process with the sheet metal loaded.

Figure 3.8: Shows the mass spectrometer machine (Taken with permission from Roofing Rolling Ltd.

The material preparation involved a meticulous cleaning process using sandpaper ensuring the removal of any surface contaminants. Subsequently, the prepared material was inserted into the machine, following the guidelines. This preparation procedure was crucial to ensure accurate and reliable results in determining the material composition using the mass spectrometer.

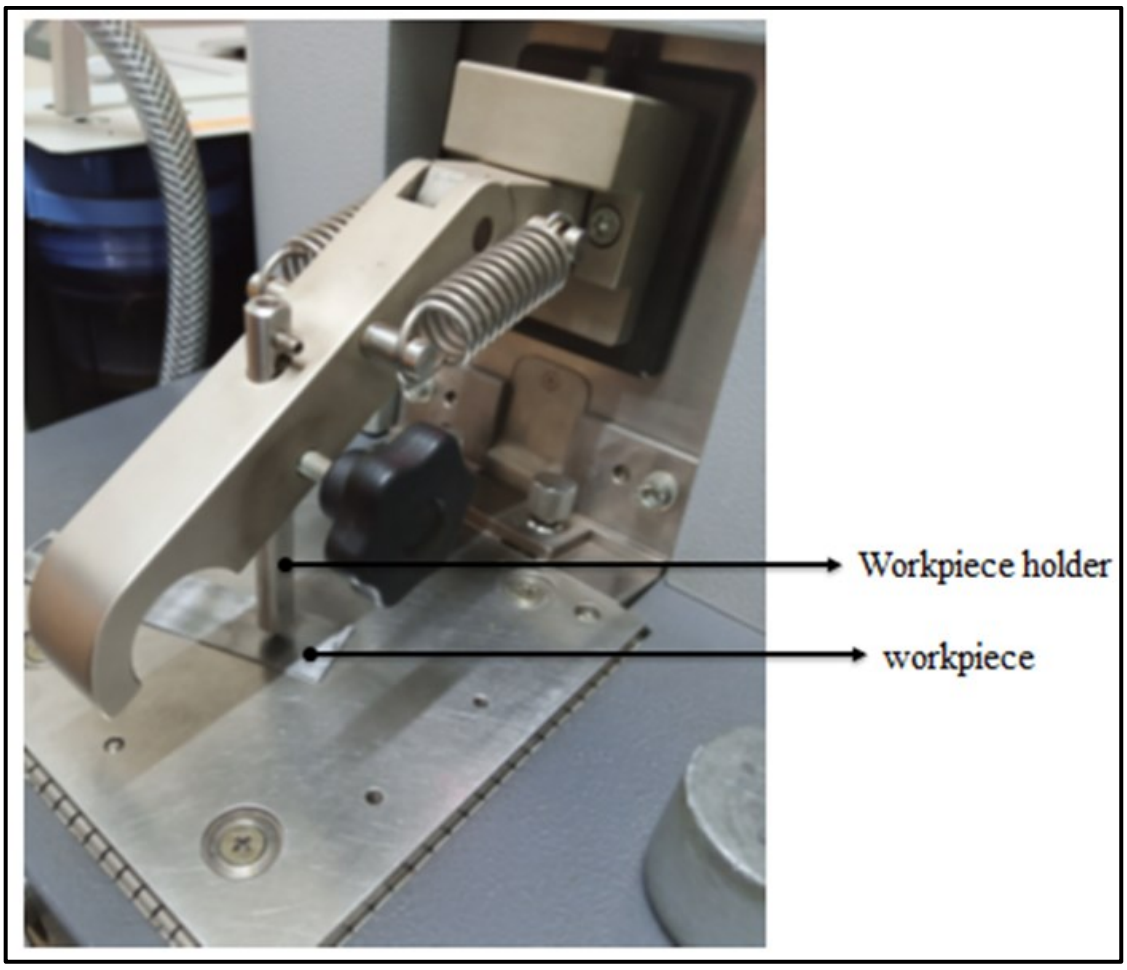

Figure 3.9: Showing testing of the composition of the material with permission from Roofings Group.

3.5 Qualitative Evaluation of Weld Quality Attributes.

3.5.1 Non-Destructive Testing.

Qualitative testing, as a non-destructive method, offers the advantage of assessing spot welds without causing damage to the component. This method of testing was intended to establish whether there were flaws, discontinuities or porosities within the nugget that could affect the quality of the spot weld and hence its performance.

3.5.1.1 Dye PenetrantMethod.

For this test, five spot-welded specimens were subjected to a specific procedure. The testing method involved the utilization of three distinct materials; the cleaner, the penetrant and the developer. The set of materials used is shown in Figure 3.10.

These materials play essential roles in the overall process. The cleaner serves to prepare the surface by removing any contaminants ensuring a clean and receptive surface for inspection. The penetrant was then applied to the surface infiltrating any potential discontinuities in the weld. Finally, the developer brings out and highlights these penetrant-filled flaws allowing for a thorough visual examination. This three-step process using designated materials forms a crucial part of the overall testing methodology facilitating the identification of potential surface defects in the spot-welded specimens.

Figure 3.10: A set of dye penetrant that was used in dye penetrant method.

3.5.1.2 X-ray Method

This method of testing is used to inspect materials for hidden flaws or discontinuities by applying short wavelength electromagnetic radiation to penetrate a material under test. The

test sample is placed between the radiation generator and the sensitive film. The intensity of the radiation that penetrate the test piece is captured by the radiation sensitive film. The radiation that passes through the test piece is captured by the film and forms a shadow-graph. The film darkness varies with the amount of radiation reaching the film through the test piece.

The dark areas indicate more exposure while the lighter ones indicate less exposure. The variation in exposure reveals the presence of any flaws or discontinuities in the material.

Figure 3.11: X-ray equipment

Experimental Design for Evaluating the Effect of the Process Parameters on the Quality of Spot Welds.

To examine the impact of the parameters on the quality of spot welds, nine experiments were conducted. For each parameter, three factor levels with increasing values shown in the Table 3.2 below were considered.

Table 3.2: Shows the values of the welding parameters used.

S/N	Electrode force (Kgf)	Welding current (kA)	Weld time (Cycles)
1	7	8	10
2	10	18	20
3	13	30	30

For the first set of experiments, three specimens were prepared using increasing values of the welding current namely; 7, 10 and 13kA while keeping the other parameters constant for the weld cycle and electrode force at 20 cycles and 18kgf respectively.

After welding, the three specimens were examined using the X-ray equipment above to establish the size of the nugget and its form. The second set of experiments was conducted using increasing values of weld time namely; 10, 20 and 30 cycles while the other two parameters constant, welding current at 10A, and electrode force at 18kgf. The third set of experiments was conducted using increasing values of the electrode force namely; 8, 18 and 30kgf, while keeping the welding current and weld time constant at 12A and 20 cycles respectively.

Method used to measure the diameter of the nugget from the X-ray film

Using the X-ray films developed from the experiments, the diameter of the nugget was measured as shown in Figure 3.12 below;

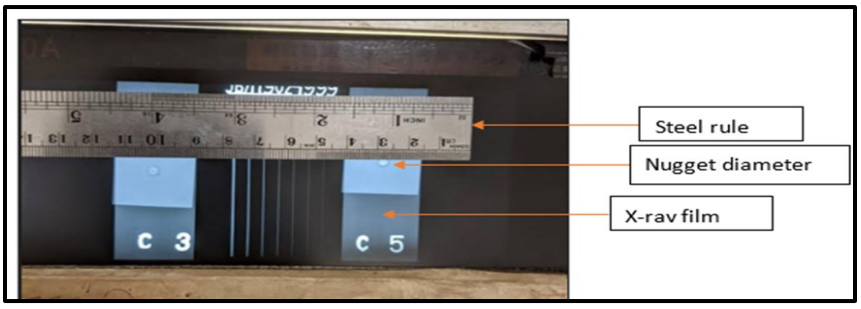

Figure 3.12: Measurement of the nugget diameter from the X-ray film

3.5.2 Destructive Testing Method of Qualitative Evaluation.

In qualitative evaluation, destructive testing stands out as the predominant method for assessing spot welds with a particular focus on two primary techniques peel and chisel tests as emphasized by existing literature, (Rawal, Kolhapure, Sutar, & Shinde, 2016). In the context of this study, the peel test was used to evaluate the quality of spot welds.

The method is a widely recognized and applied method involving the deliberate separation of welded materials to assess the strength and integrity of the joint. This method provides crucial insights into the bonding quality and structural performance of spot welds, contributing valuable data to the overall evaluation of their effectiveness and durability.

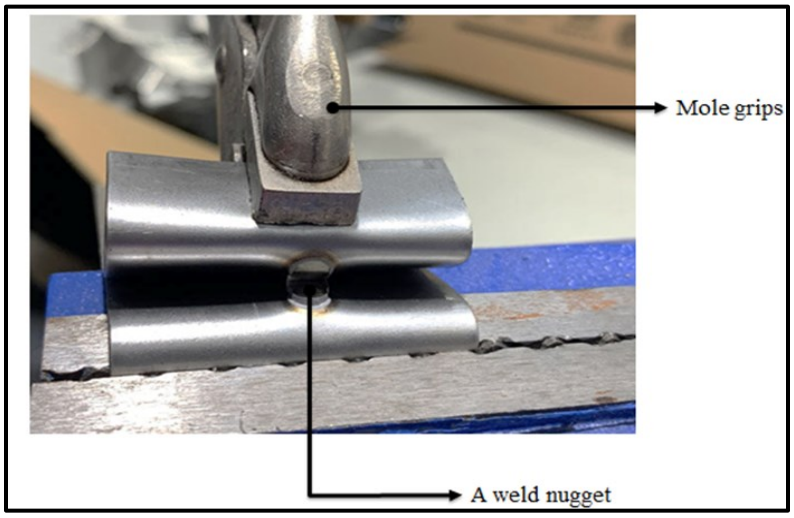

Figure 3.13: Destructive testing using peel test method (BWS, 2019).

Using the peel test method, figure 3.13 above the specimen underwent deliberate destruction by peeling apart one piece of the welded sheet metal at a time to verify the quality of the joint. Employing a monkey plier for peeling off one piece and a vice for holding the other, one part of the welded metal was systematically peeled away, showcasing the destructive nature of this testing method. This procedure allowed for a

detailed examination of the welded joint, providing insights into the bonding strength and integrity of the spot weld.

3.6 Quantitative Evaluation of Weld Quality Characteristics

Quantitative evaluation of spot welds involves a comprehensive understanding of their load-bearing characteristics, encompassing measurements of size of the weld nugget, nugget penetration, and weld strength.

This quantitative assessment employs destructive testing methods wherein a completed weld undergoes physical destruction to evaluate its mechanical and physical attributes. Destructive testing is carried out until the specimen's failure providing insights into its performance under different loads. Various destructive testing methods including sectioning or breaking the welded component are utilized to measure mechanical and physical characteristics such as nugget diameter penetration depth and weld strength. In this study the focus was specifically on evaluating weld strength and nugget diameter as key quantitative parameters.

3.6.1 Determination of the Nugget Diameter

Two approaches were used to determine the nugget diameter as explained below. The first approach was by taking the measurements directly on the spot welded specimen as shown in the Figure 3.14. Following the completion of the tensile testing of the workpiece, it was securely placed in a vice and entirely peeled off to fully expose the nugget. Subsequently, the exposed nugget underwent measurement using a vernier caliper shown in Figure 3.14, and average values for the longitudinal and vertical measurements were determined. This particular process aimed to precisely quantify and record the

dimensions of the nugget, providing accurate data for the subsequent quantitative evaluation of the spot welds.

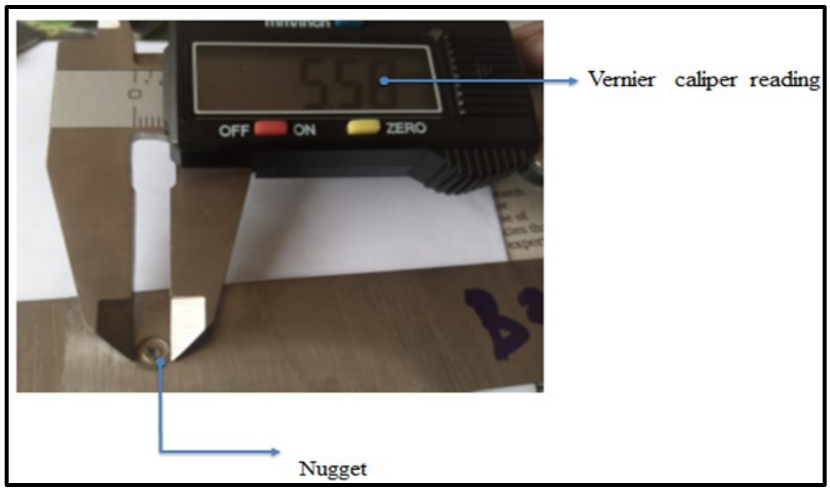

Figure 3.14: shows direct measurement of the nugget using a digital Vernier caliper.

3.6.2 Determination of the Strength of the Spot Weld

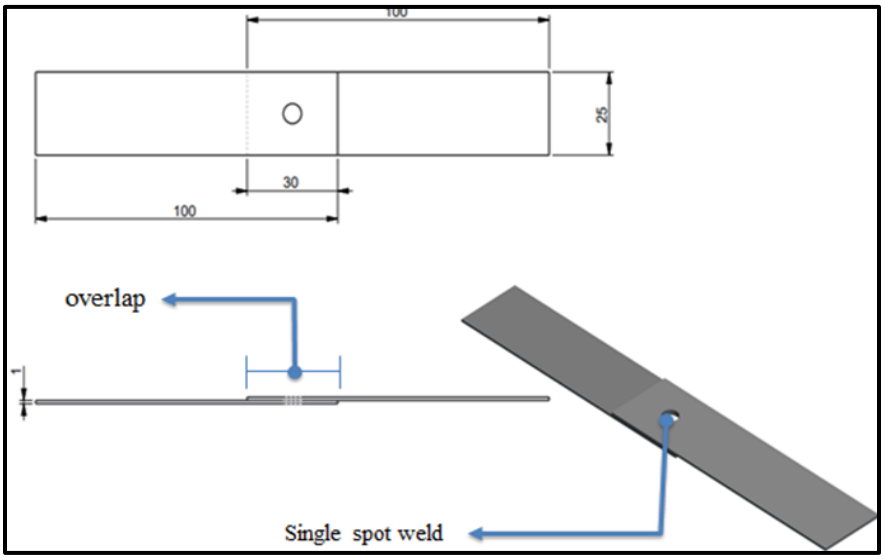

Figure 3.15: CAD of the geometry of the specimen designed as per the AWS standard.

For this study, samples consisting of 1 mm thick strips measuring 100 mm x 25 mm as shown in the Figure 3.15 were precision-cut using a shearing machine.

The arrangement of these strips followed a specified pattern. Spot welding of the specimens was conducted utilizing a 32KVA 50Hz pedestal-type RSW machine. The process involved manipulation of different parameters, in accordance with the experimental design outlined earlier. Following the welding procedure, the specimens were inserted into the upper and lower jaws of a tensile testing machine. The specific tensile testing machine employed in this study was a model UTN/E-100 with a maximum load capacity of 1000 KN, sourced from the Roofing Group Limited. The machine was activated, and the specimen was pulled apart until failure occurred. The strength values at the point of failure were recorded through the computer interface connected to the testing machine. Figure 3.16 shows a screenshot of the plotting of the graph from the machine results.

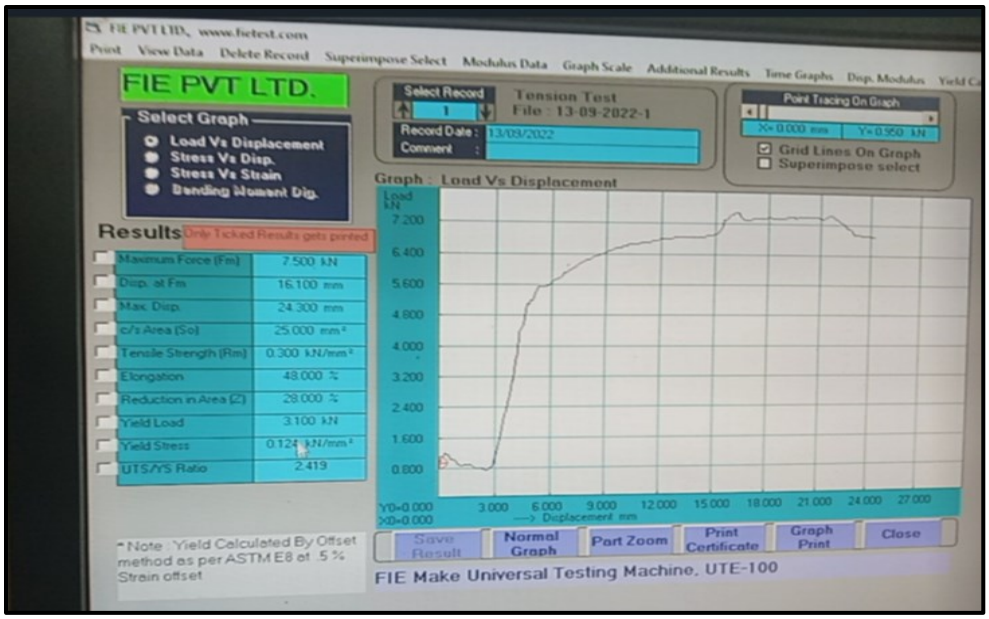

Figure 3.16: Shows a screenshot of the results of the tensile test and plotting of the graph.

3.7 Experimental Design.

3.7.1 Heat Generation in Resistance Spot Welding.

Heat generated during RSW is influenced by three key factors: welding current, contact

resistance and welded time. To ensure high-quality welds, it is essential to effectively control these parameters. The equation governing the heat generation in this process is as follows, (Zhao, Yan, Xing, Chen, & Jiang, 2020):

$$Q = I^2RT \quad \text{.....(Eqn 1)}$$

Where:

T = Time of current flow in seconds
R = Resistance of the work piece (Ω)
I = current in Amps and
Q = heat generated in Joules

3.7.2 Experimental Design for Evaluating the Effect of Process Parameters on Spot Welds Quality.

To examine the impact of parameters on nugget diameter and weld strength, the Taguchi method of experimental design was employed. The parameters namely welding current, electrode force and weld time were chosen for investigation with each parameter having five considered levels. The values for the welding current considered varied from 6 to 10A, weld time was varied from 10, 15, 20, 25 and 30 cycles while electrode force was increased from 289, 320, 380, 440 and 500 Kgf. The specific details of the factor levels for each parameter are provided in the Table 3.3 below:

Table 3.3: Factor levels for the experimental design

Factor Levels	Welding Current (A)	Weld Time (Cycles)	Electrode Force (Kgf)
1	6	10	280
2	7	15	320
3	8	20	380
4	9	25	440
5	10	30	500

In this experiment, the values for the electrode force in the table were adjusted using the following formula:

Adjusted value = ((A-200))/10 ..... (Eqn 2)

Where A represents the initial electrode force as shown in the table 3.3.

The application of this formula resulted in new values for the electrode force shown in table 3.4 below. This adjustment was implemented to derive modified values for the electrode force introducing a systematic variation for the experimentation process.

Table 3.4: Shows the adjusted values of the electrode force

Factor Levels	Welding Current (A)	Weld Time (Cycles)	Electrode Force (Kgf)
1	6	10	8
2	7	15	12
3	8	20	18
4	9	25	24
5	10	30	30

3.6.1.1 Evaluating the Effect of Welding Current on Weld Quality.

In this experiment, there were five sets of tests conducted, with each set comprising of 5 specimens. In each set, the welding current was kept constant while the weld time and

electrode force were increased. The electrode force and weld time were increased in steps of 6kgf and 5 cycles respectively. In total, there were 25 tests carried out.

3.6.1.2 Evaluating the Effect of Weld Time on Weld Quality.

During this experiment, five sets of tests were executed, and each set consisted of 5 specimens. Within each set the weld time was maintained at a constant value while the welding current and electrode force were systematically increased. Specifically, the electrode force was elevated in increments of 6 Kgf and the welding current was increased in steps of 1A. Consequently, a total of 25 tests were conducted to comprehensively investigate the effects of varying parameters on the experimental outcomes. It is important to note that the unit used for weld time is a cycle where 1 cycle equates to 0.014 seconds. This information provides clarity on the temporal aspect of the welding process.

3.6.1.3 Evaluating the Effect of Electrode Force on Weld Quality.

In this experiment, there were five sets of tests conducted, with each set comprising of 5 specimens. In each set, the electrode force was kept constant at 10, 15. 20. 25 and 30Kgf while the welding current and weld time were increased from 6 to 10A and 10 to 30 cycles respectively. The welding current and weld time were increased in steps of 1A and 5 cycles respectively. In total, there were 25 tests carried out

CHAPTER FOUR: RESULTS AND DISCUSSION

This chapter presents the results obtained from experiments done to evaluate the effect of the spot-welding parameters (welding current, weld time and electrode force) on the quality of the spot weld expressed in terms of the weld strength, nugget diameter. The experiments conducted were both non-destructive (x-ray) and destructive (tensile). The optimum parameters were obtained.

4.1 Results for Testing the Chemical Composition of the Steel Sheet

Two samples were tested and Table 4.1 below shows the average values of the results of the test for the chemical composition of the material.

Table 4.1: Main properties of copper

C %	Si %	Mn %	P %	S %	Cr %	Mo %	Ni %	Al %	
0.09	0.0206	0.125	0.197	0.0045	0.0301	0.001	0.0122	0.0731	0.004
Cu %	**Sn %**	**Ca %**	**B %**	**La %**	**N %**	**Sb %**	**Te %**	**Fe %**	
0.0095	0.00081	0.00037	0.00047	0.0008	0.0579	0.0041	0.0081	99.4	

The chemical composition analysis revealed that the steel under investigation falls into the category of low-carbon steel. This categorization is based on the relatively low percentages of carbon (C), typically characterized by values around 0.09%. Low-carbon steels are known for their favorable welding and forming properties, as well as their suitability for applications requiring a balance between strength and ductility. The other alloying elements present in the composition, such as silicon (Si), manganese (Mn), and

various trace elements, contribute to the overall characteristics of the steel, making it suitable for specific engineering and manufacturing purposes.

4.2 Determination of the Hardness of the Material

To assess the hardness of the material, a test piece measuring 30 mm x 75 mm was cut using a shearing machine. After cleaning with an emery cloth, the test piece was subjected to hardness testing. Measurements were obtained from eleven different points and the results are depicted in Figure 4.1 below. Direct readings from the scale yielded minimum, maximum, and average hardness values of 48, 49.5, and 51, respectively. The average value of 49.5 was taken as the hardness value of the material.

The hardness testing indicated variations across different points with values ranging from 48 to 51. The minimum and maximum values represent the hardness extremes observed while the average hardness provides a central tendency measure. This variation may be attributed to factors such as material composition and manufacturing processes.

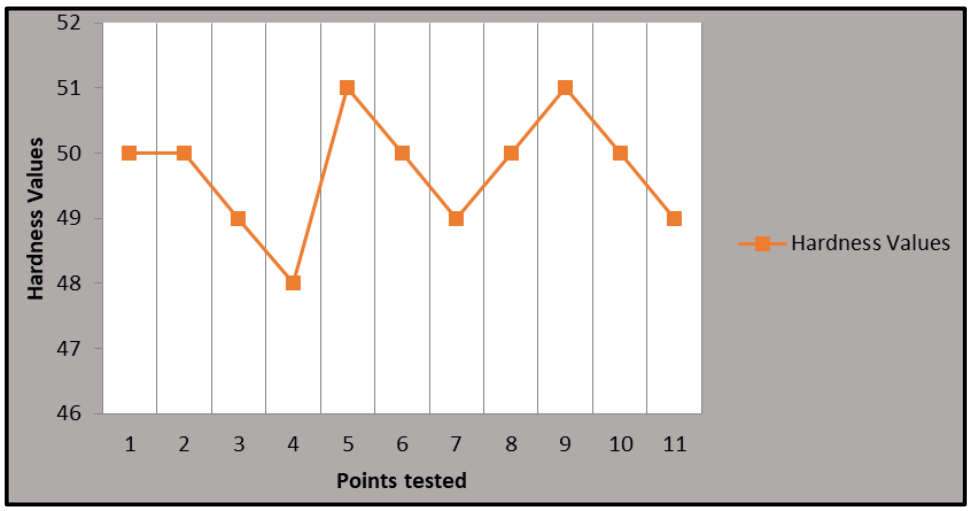

Figure 4.1: Hardness values obtained from the eleven points tested

Overall, understanding material hardness is crucial for predicting its behavior in different applications contributing valuable insights for further analysis and experimentation in this study.

4.2.1 Determination of the Mechanical Properties.

Strength and Elongation

Three pieces of the test material measuring 50 mm x 300mm were cut and inserted into the tensile testing machine one after another and were each subjected to a tensile force until failure occurred. The values of the tensile strength and elongation at failure were obtained from the readings on the computer connected to the machine. The average values obtained from the three readings for the tensile strength and elongation were 0.166 KN/mm2 and 48.73% respectively as shown in table 4.2 below. The values of the properties obtained were; Hardness 46.5kgf, Maximum Tensile Strength 0.3KN/mm2, Elongation 49% and Maximum Force 7.5kN.

Table 4.2: Details of the mechanical properties of the material used.

Hardness (Kgf) (Kgf)	**Maximum tensile strength** (kN/mm^2)	**Elongation** (%)	**Maximum force** (kN)
46.5	0.3	49	7.5

4.3 Non-Destructive TestResults

4.3.1 Results of the Dye Penetrant Test Method

In the dye penetrant method, the procedure began with the cleaning of the five workpieces. A chemical was applied by spraying specifically at the spot welds, followed by thorough cleaning using a dry cotton cloth. Subsequently, the penetrant was applied, Figure 4.2, to

the workpieces through a spraying process, allowing a ten-minute period for the material to effectively penetrate any potential discontinuities in the welds. Following this penetration stage, the work pieces underwent cleaning using a wet cloth rinsed in the cleaner to remove excess penetrant.

After the cleaning process, a developer was then sprayed onto the work pieces as shown in the Figure 4.3.

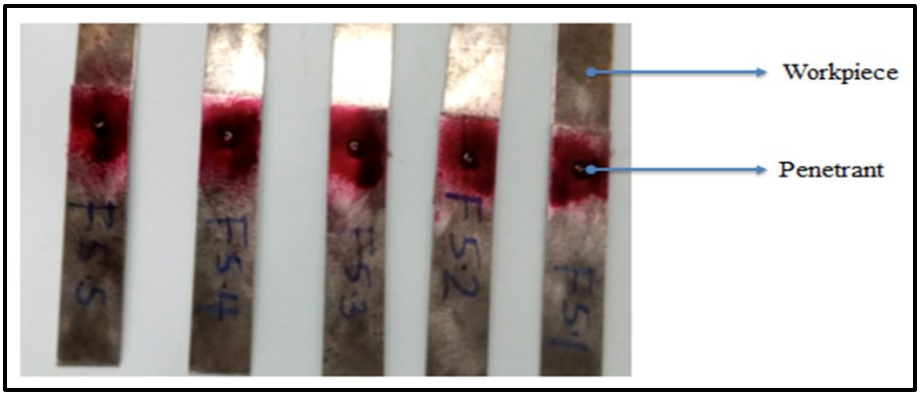

Figure 4.2: Penetrant applied to the work pieces.

The developer helps to ensure that any discontinuity in the spot weld is visible. This step-by-step methodology, involving the careful application of chemical agents and adequate waiting periods, ensures a comprehensive examination of the spot-welded specimens through the dye penetrant method.

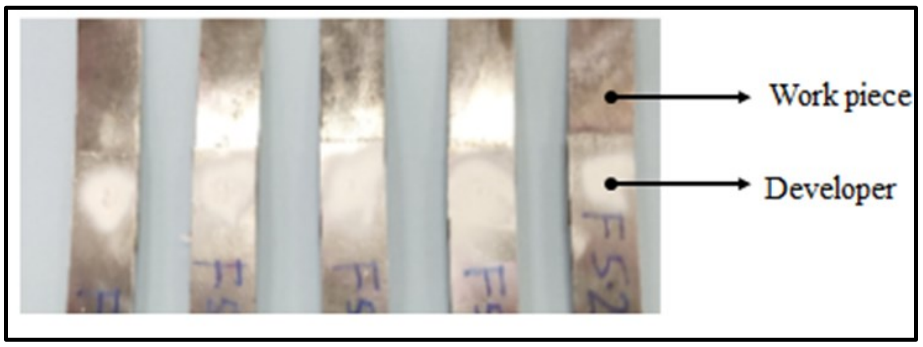

Figure 4.3: Developer applied to the workpieces.

The examination of the workpieces revealed a notable absence of surface cracks. The thorough inspection conducted through various testing methods did not detect any visible indications of cracks on the surfaces of the specimens.

This finding underscores the integrity and soundness of the welded joints, indicating a spot of successful welding with no apparent surface defects.

4.3.2 Results for the X-Ray Test Method

The equipment used for this evaluation method was a RIGAKU Industrial X-Ray apparatus equipment model, Radio flex 300 EGS3 shown in the Figure 3.11. The X-ray radiations were produced by a radioflex 300EGS3 generator. The source and object distance were 600mm and the film distance was 605mm. A single wall single image technique was used during the shooting process. The radiations were generated for 0.1 minute using 160kV and each cassette contained one film. KODAK AA 400 films were processed manually using an x- ray film fixer and developer. Each step of the processing procedure took 5 min. A film illuminator was used to aid in the evaluation of the films. Observations were done visually.

4.3.3 Determination of the Effect of Welding Current on the Quality of the Spot Weld

The experiment was carried out using increasing values of welding current of 7, 10 and 13 kA while keeping the weld time and electrode force constant at 20 cycles and 18 Kgf respectively as shown in the table 4.3 below.

Table 4.3: Showing average results of the tensile strength and elongation

S/N	Welding Current (A)	Welding Time (Cycles)	Electrode Force (kgf)
1	7	20	18
2	10	20	18
3	13	20	18

The results of the specimen for the three experiments were represented by A1, for 7A, 20 Cycles and 18kgf, A3 for 10A, 20 cycles and 18kgf, and A5 for 13A, 20 cycles and 18kgf respectively. The x-ray films developed from the three experiments are shown in Figure 4.4.

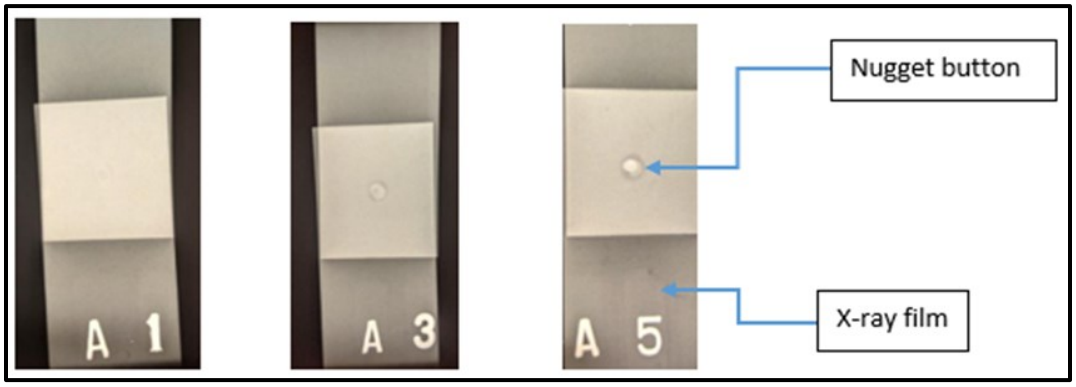

Figure 4.4: Showing the x-ray films of the first set of experiments.

From the first experiment B1 using the parameters, 10 cycles, 10A and 18kgf, results show the nugget was not very clear implying that the weld nugget formation time was not adequate. The diameter of the nugget measured was 6.7 mm. By increasing weld time to 20 cycles, B3, the weld nugget became clearer. However, there were defects observed towards the inner most part of the nugget. The average value of the diameter of the nugget measured was 7.0 mm. B5 shows the result of increasing the weld time to 30 cycles. The nugget together with all the zones were very clear and there were no defects observed. The average value of the diameter of the nugget measured was 7.3 mm. Increasing weld time

increases the quality of spot weld. However, increasing weld time without sufficient welding current does not produce a good spot weld and this could have caused the condition for B3. The best welding parameters that gave a quality spot weld for this experiment were therefore 10A, 30 cycles and 18 kgf.

4.3.4 Determination of the effect of weld time on the quality of the spot weld.

This experiment was carried out using increasing values of electrode force 8, 18 and 30 kgf while keeping welding current and weld time constant at 12 A and 20 cycles respectively as shown in Table 4.4. The results of the specimen for the three experiments were represented below by B1, for 8 kgf, 12 A and 20 cycles, B3 for 18 kgf, 12 A and 20 cycles, and B5 for 30 kgf, 12 A and 20 cycles respectively. The x-ray films developed from the three specimens are shown in the Figure 4.5.

Table 4.4: Showing the experimental design for the second set of experiments.

S/N	Welding Time (Cycles)	Welding Current (A)	Electrode Force (kgf)
1	10	10	18
2	20	10	18
3	30	10	18

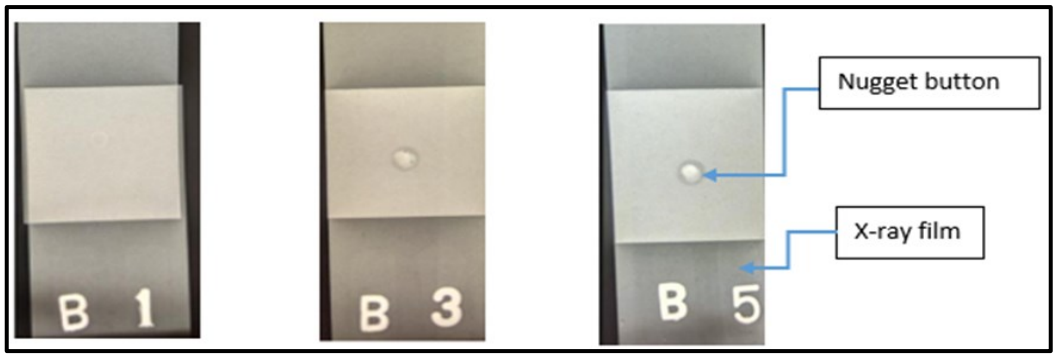

Figure 4.5: Showing the x-ray films of the second set of experiments.

From the first experiment B1 using the parameters, 10 cycles, 10A and 18kgf, results show the nugget was not very clear implying that the weld nugget formation time was not adequate. The diameter of the nugget measured was 6.7 mm. As the weld time was increased to 20 cycles, B3, the nugget became clearer. However, there were defects observed towards the innermost part of the nugget and the average diameter of the nugget measured was 7.0 mm. B5 shows the result of increasing the weld time to 30 cycles. The nugget together with all the zones were very clear and there were no defects observed. The average diameter of the nugget measured was 7.3 mm. Increasing the weld time increases the quality of the spot weld. However, increasing the weld time without sufficient welding current does not produce a good spot weld and this could have caused the condition for B3. The best welding parameters that gave a quality spot weld for this experiment were therefore 10A, 30 cycles and 18 kgf.

4.3.5 Determination of the Effect of Electrode Force on the Quality of Spot Weld

This experiment was carried out using increasing values of electrode force 8, 18 and 30 kgf while keeping the welding current and weld time constant at 12 A and 20 cycles respectively as shown in Table 4.5 below.

Table 4.5: Showing the experimental design for the second set of experiments.

S/N	Electrode Force (kgf)	Welding Current (A)	Welding Time (Cycles)
1	8	12	20
2	18	12	20
3	30	12	20

The results of the specimen for the three experiments were represented below by C1, for 8 kgf, 12 A and 20 cycles, C3 for 18 kgf, 12 A and 20 cycles, and C5 for 30 kgf, 12 A and 20 cycles respectively. The x-ray films developed from the three specimens are shown in the Figure 4.6 below.

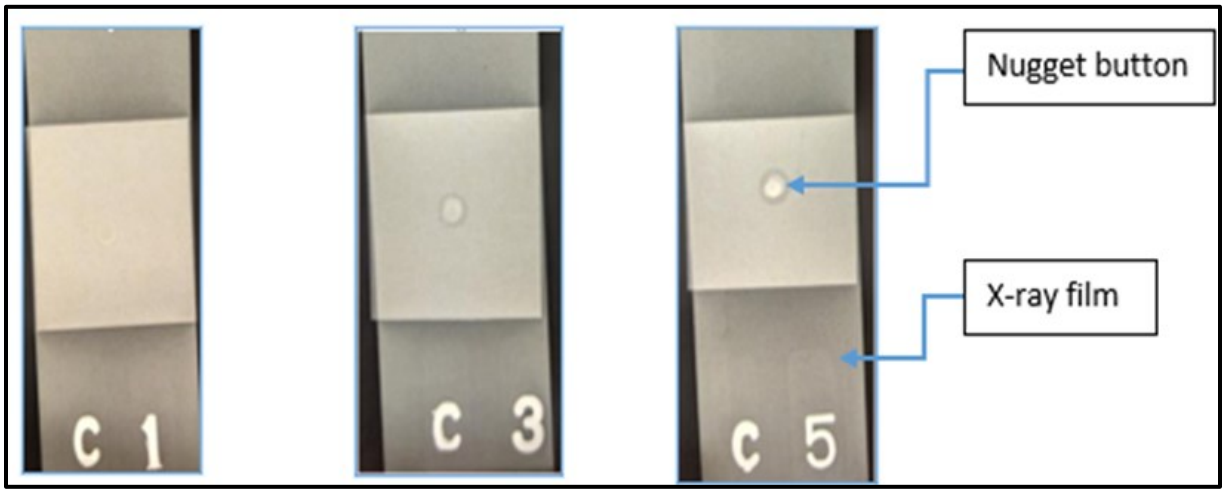

Figure 4.6: Showing the x-ray films of the third set of experiments.

Results of the first experiment, C1, with 8 kgf, 12 A and, 20 cycles showed a nugget which was small and faint with no defects observed. The average diameter of the nugget measured was 6.8 mm. Low electrode force is associated with heat being conducted away from the weld area leaving no chance for nugget formation hence a poor quality spot weld.

When the electrode force was increased, C3, to 18 kgf keeping the other parameters constant, the visibility of the nugget increased and the average diameter of the nugget measured was 7.2 mm and there were no defects observed. When electrode force was increased further to 30 kgf, C5, there was a small improvement in the clarity the average diameter of the nugget measured was 7.3mm.

Increasing the electrode force was observed to cause no significant increase in the size of the spot weld nugget because of the increase in electrical resistance at the contact surface prohibited the nugget formation. The best operating parameters that gave a good quality spot weld for this experiment were 30kgf, 12 A and 20 cycles.

4.4 Destructive tests

The peeled samples are indicated in Figure 4.7 below. It is noteworthy that failure did not occur directly at the joint but instead occurred around the heat-affected zone. This observation suggests that the spot-welded joint exhibited strength but there was a weakness specifically in the heat-affected zone. The location of the failure around this zone implies that the welding process successfully created a robust joint but the heat-affected zone might re- quire further attention or optimization to enhance its overall strength and performance. This insight into the failure pattern contributes valuable information for refining and improving the welding process in future applications.

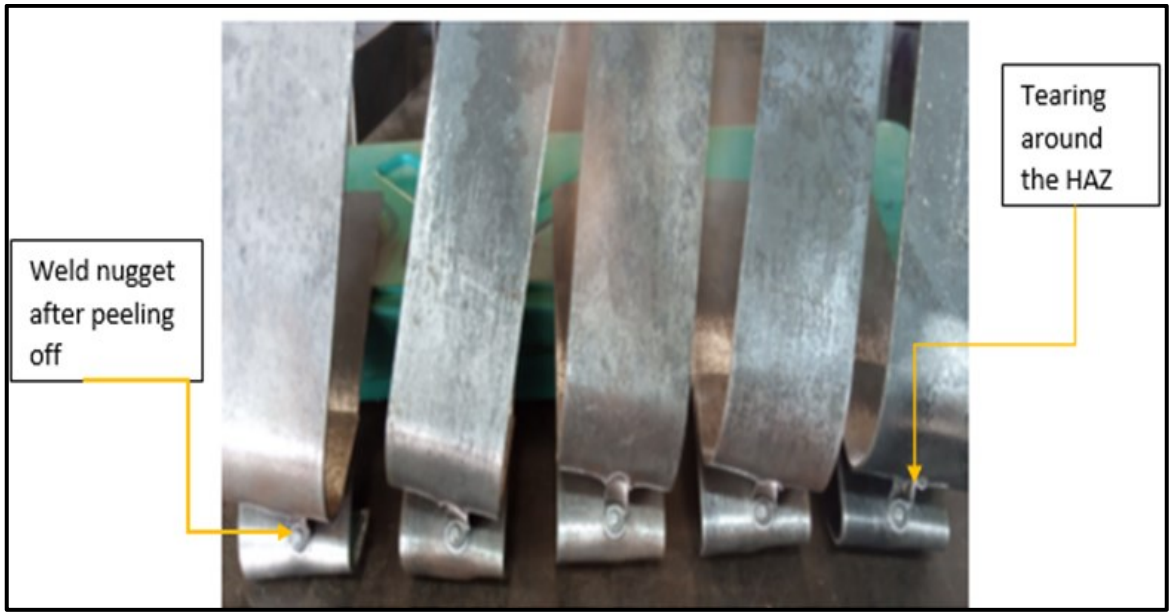

Figure 4.7: Test pieces after the peel test

4.4.1 Determination of the Effect of Welding Current on Weld Quality Attributes.

Table 4.6: Showing average values of weld strength and nugget diameter using welding current as the independent variable

Welding current (A)	Electrode Force (Kgf)	Weld Time (Cycles)	Weld strength (KN)	Nugget Diameter (mm)
6	8	20	3.71	6.84
7	8	20	4.01	6.96
8	8	20	4.51	7.1
9	8	20	4.63	7.84
10	8	20	4.71	7.54

4.4.2 Determination of the Effect of Weld Time on Weld Quality Attributes.

Table 4.7 below shows the average values of the weld strength and nugget diameter computed from the 25 experiments.

Table 4.7: Experimental design layout for evaluation the effect of weld time on weld quality.

S/N	Welding Time (Cycles)	Electrode Force (Kgf)	Weld Current (A)	Weld strength (KN)	Nugget Diameter (mm)
1	10	8	6	3.21	6.32
2	15	12	7	3.55	6.40
3	20	18	8	3.34	6.92
4	25	24	9	3.76	7.14
5	30	30	10	3.9	7.18

4.4.3 Determination of the Effect of Electrode Force on Weld Quality Attributes.

Table 4.8 below shows the average values of the weld strength and nugget diameter obtained.

Table 4.8: Orthogonal array for evaluating the effect of electrode force on weld quality.

S/N	Electrode Force (Kgf)	Welding current (A)	Weld Time (Cycles)	Weld strength (KN)	Nugget Diameter (mm)
1	8	6	10	3.71	6.84
2	12	7	15	4.01	6.96
3	18	8	20	4.51	7.1
4	24	9	25	4.63	7.84
5	30	10	30	3.25	7.54

4.4.1.1 Effect of Welding Current on Weld Strength.

The influence of welding current on weld strength was evaluated by plotting values of welding current against corresponding weld strength. Figure 4.8 below is a graphical representation which visually depicts the relationship between weld strength and welding current. This graphical representation provides insights into how changes in welding current impact the resulting weld strength facilitating a clearer understanding of the observed behavior of the welding process. The values of welding current against weld strength were plotted and shows the behavior of the weld strength against increasing values of the welding current. Figure 4.8 below shows that as welding current increased, weld strength increased suddenly until it reached a value of 4.5 kN.

After that, there was a gradual increase in the weld strength until a maximum value of 4.71 kN was reached. The current was 10 A. This observed behavior offers valuable insights into the relationship between welding current and resulting weld strength, showcasing distinct phases of response in the welding process.

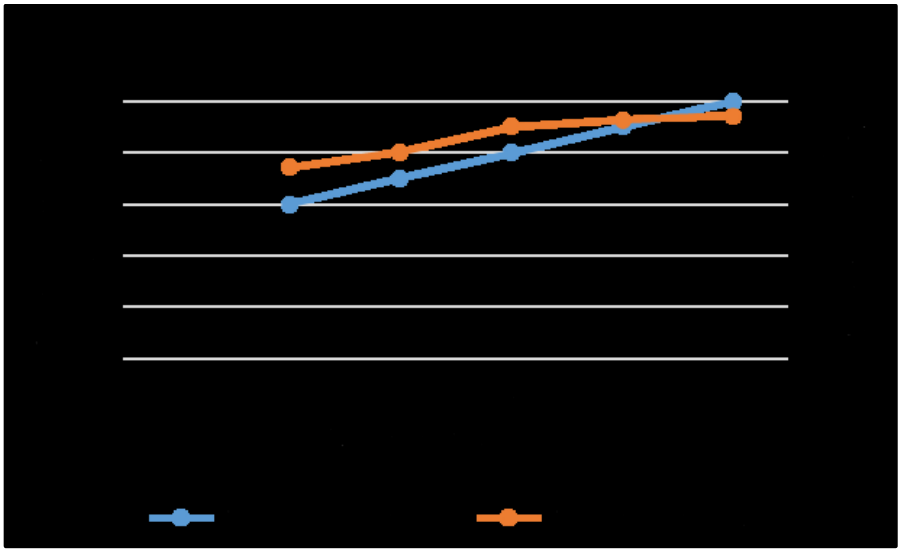

Figure 4.8: Effect of welding current on weld strength

4.4.1.2 Effect of Welding Current on Nugget Diameter.

Using average values of welding current and nugget diameter from Table 4.8 above a graph was plotted and the results are shown in Figure 4.9 below. The chart shows that as welding current increased to 8A, the nugget diameter increased until it reached a maximum value of 7.8 mm. It then dropped to 7.4 mm when the current increased to 10A. The reason for this decrease in nugget diameter is that during spot welding of the specimen, some expulsion was observed, which led to the loss of molten metal due to splashing, which could not allow the formation of a good size of nugget diameter. This also explains the loss in strength observed in Figure 4.8 above.

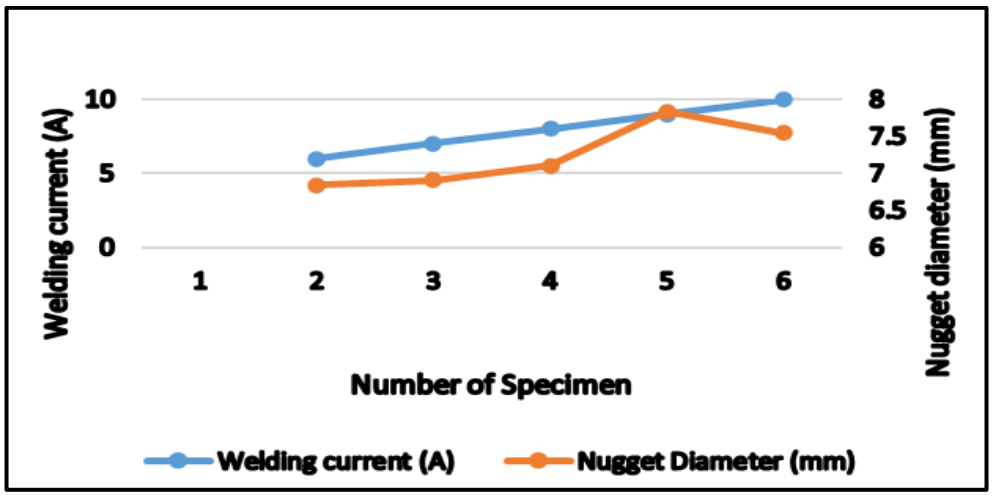

Figure 4.9: Variation of nugget diameter with increasing welding current

4.4.4 Determination of the Effect of Weld Time on Weld Quality Attributes.

From the twenty five experiments conducted, using weld time as the independent variable, values of weld strength and nugget diameter were obtained and analyzed to establish the effect of changing weld time on the quality of the spot weld in terms of weld strength and nugget diameter. From the results, average values of weld strength and nugget diameter were calculated and table 4.9 shows the values obtained.

Table 4.9: Table showing the average values of the weld strength and nugget diameter.

Welding Time (Cycles)	Electrode Force (Kgf)	Weld Current (A)	Weld strength (KN)	Nugget Diameter (mm)
10	18	8	3.21	6.33
15	18	8	3.55	6.4
20	18	8	3.34	6.92
25	18	8	3.76	7.14
30	18	8	3.87	7.18

4.4.2.1 Effect of Weld Time on Weld Strength

From Table 4.9 above, a graph was plotted to show the behavior of weld strength against increasing values of weld time and the results are displayed on graph shown in figure 4.10 below. It has already been indicated that the strength of the weld is proportional to the size of the weld nugget. Increasing the weld nugget leads to a stronger weld. At the same time, increasing the weld time leads to an increase in the weld nugget because as weld time increases, more time is allowed for the molten metal to form and solidify leading to a bigger diameter of the nugget and therefore a stronger weld.

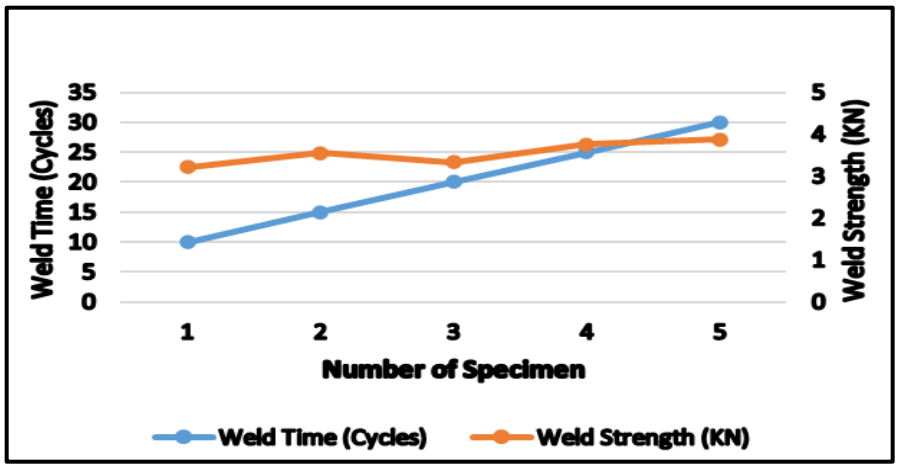

Figure 4.10: Graph illustrates the effect of weld time on weld strength.

4.4.2.1 Effect of Weld Time on the Nugget Diameter

From the graph shown in Figure 4.11, as weld time increased, the nugget diameter increased. This is because weld time is directly proportional to the heat being generated. Increasing weld time leads to an increase in heat generated. In addition, increasing weld time allowed time for the contact surface temperature to increase leading to more melting of the contact zone. If the increase in weld time is proportional to welding current, no spatter occurs, thus

allowing for equilibrium of the molten pool leading to an increase in nugget diameter.

From the graph, a maximum value of 7.2mm for nugget diameter was reached with a weld time of 30 cycles.

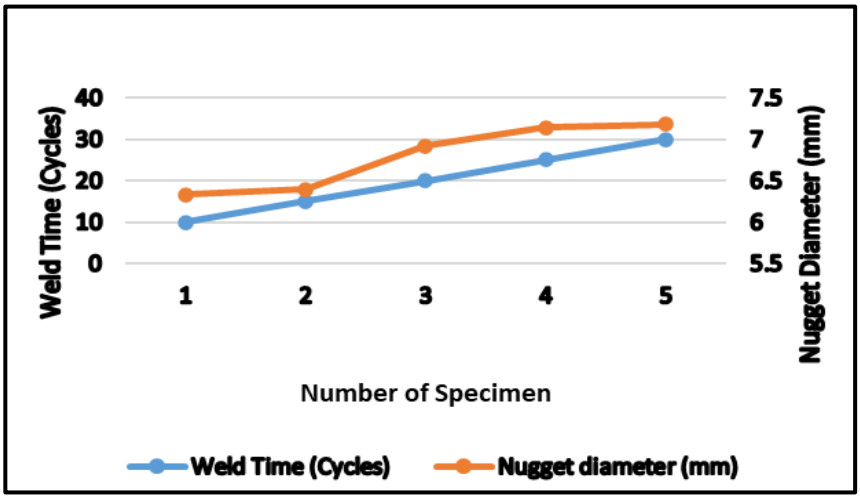

Figure 4.11: Showing the effect of weld time on nugget diameter.

4.4.5 Effect of Electrode Force on Quality of Spot Weld.

From the twenty-five tests conducted average values were obtained for the dependent and independent variables and table 4.10 below shows the results. The average values for welding current and weld time were constant at 7A and 20 cycles respectively.

Table 4.10: Showing the average values obtained from the tests conducted.

Welding Current (A)	Weld Time (Cycles)	Electrode force (Kgf)	Weld strength (KN)	Nugget Diameter (mm)
7	20	6	4.57	6.56
7	20	12	4.55	6.64
7	20	18	4.5	6.62
7	20	24	4.44	6.33
7	20	30	4.4	5.5

The graphs show that the weld strength decreased as the electrode force increased. As

already observed by various researchers increasing the electrode force reduces the contact resistance between the contact surfaces of the metals. This reduces the welding current which does not allow the generation of sufficient heat favoring nugget formation.

4.4.3.1 Effect of Electrode Force on the Weld Strength.

With an electrode force of 6kgf, the value of nugget diameter was 6.5 mm and slightly increased to 6.6 mm. However, as electrode force increased, it went on reducing up to 5 mm diameter corresponding to 30 Kgf. This behavior was because increasing electrode force increased the contact surface area of the faying surfaces. Since resistance is indirectly proportional to contact area as the contact area increases, resistance reduces and therefore the generated heat also decreases which makes the nugget size to keep on decreasing. This is indicated by the graph in Figure 4.12 below.

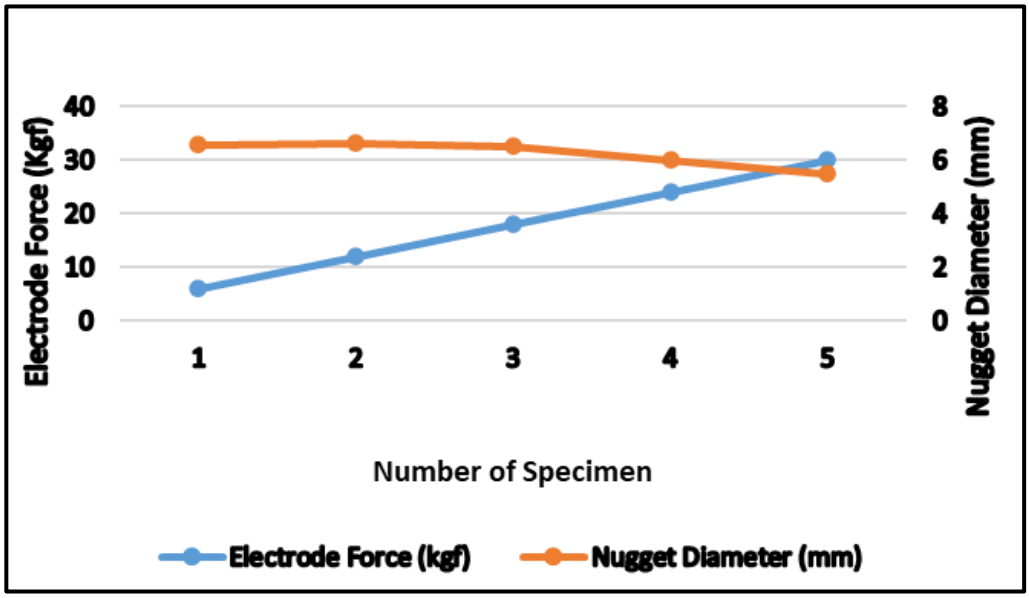

Figure 4.12: Shows the effect of electrode force on nugget diameter.

4.4.3.2 Effect of Electrode Force on the Nugget Diameter

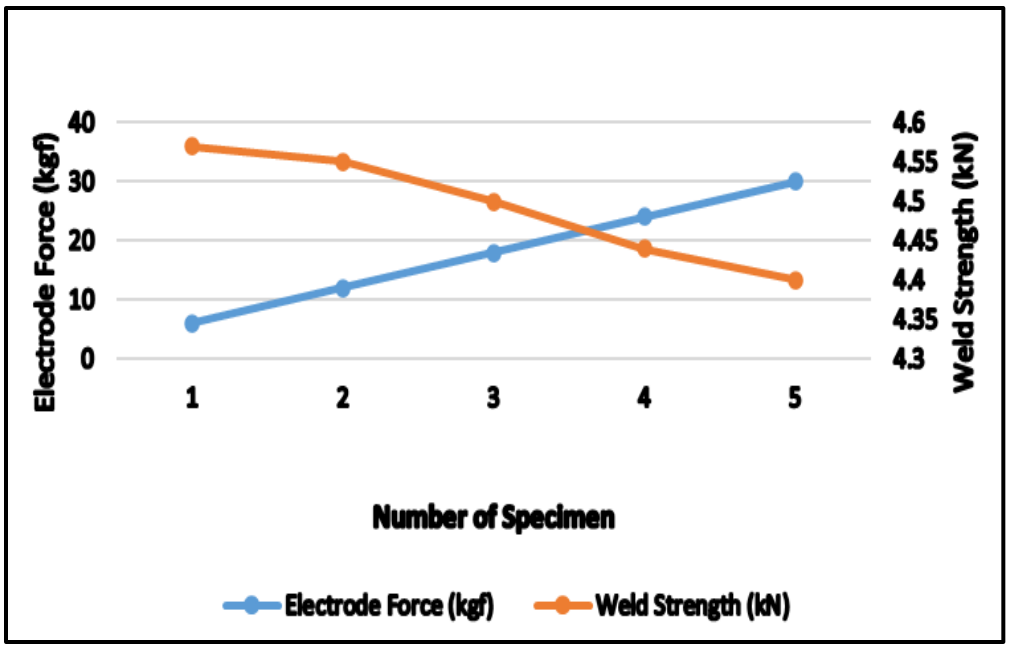

Figure 4.13: Shows the effect of electrode force on weld strength.

Figure 4.13 above shows the changes in weld strength with increasing electrode force. The weld strength reduced from 4.57kN to 4 kN corresponding to electrode force of 6 Kgf and 30 Kgf respectively.

When electrode force is low, the contact resistance is high resulting in elevated current density. This high current density generates significant heat leading to an increased melting rate of the material. Consequently, this process results in a larger diameter of the nugget and a higher value of the weld strength. On the other hand, as electrode force increases, both the contact resistance and current density decrease. This reduction in heat generation leads to insufficient melting of the material, resulting in a smaller diameter of the weld nugget and ultimately a decrease in weld strength.

4.5 The Optimal Process Parameters for Enhanced Strength of the RSW

4.5.1 Results of the Effect of Increasing Welding Current on Nugget Diameter

Figure 4.14 below shows the effect of increasing welding current on the size of the nugget diameter.

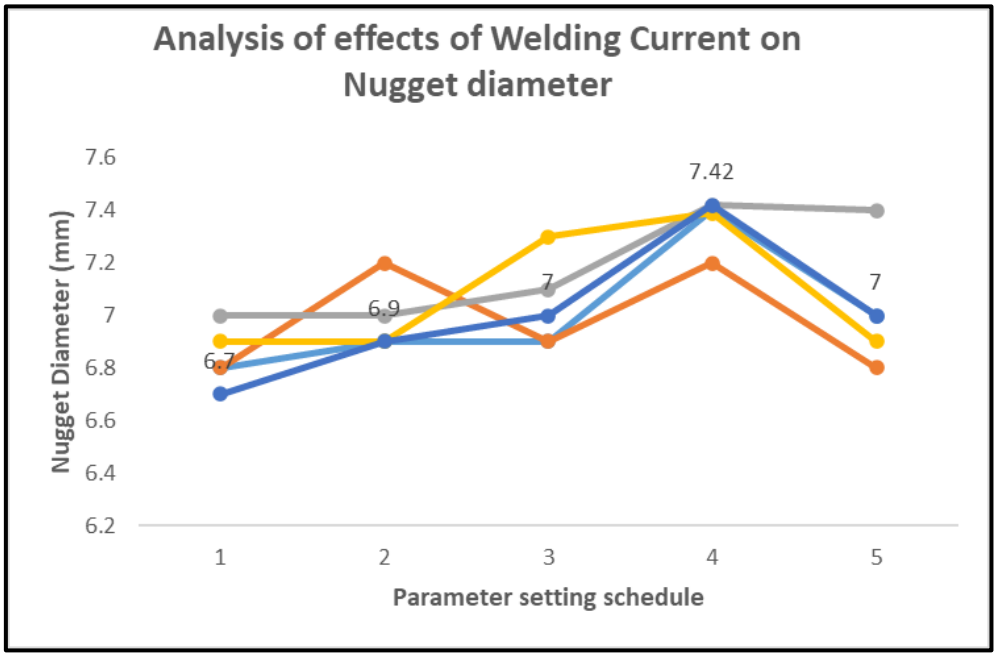

Figure 4.14: Effect of increasing welding current on nugget diameter

From the figure above, each line plot shows the results of 5 specimen tested after welding them using different welding parameters with increasing values of the welding current. The values for the different sizes of the nugget diameter are shown in table 4.11. The results shows that the highest values of the nugget diameter were 7.42mm. This corresponds to a welding current of 10A, electrode force of 18kgf and weld time of 20 cycles.

Table 4.11: The values of the nugget diameter for different parameter setting schedules.

Schedule	Size of Nugget	Diameter	(mm)		
1	6.8	6.9	6.9	7.4	7
2	6.8	7.2	6.9	7.2	6.8
3	7	7	7.1	7.42	7.4
4	6.9	6.9	7.3	7.39	6.9
5	6.7	6.9	7	7.4	7

4.5.2 Results of the Effect of Increasing Welding Current on the Strength of the Weld

Figure 4.15 below shows the effect of increasing weld time on the strength of the weld.

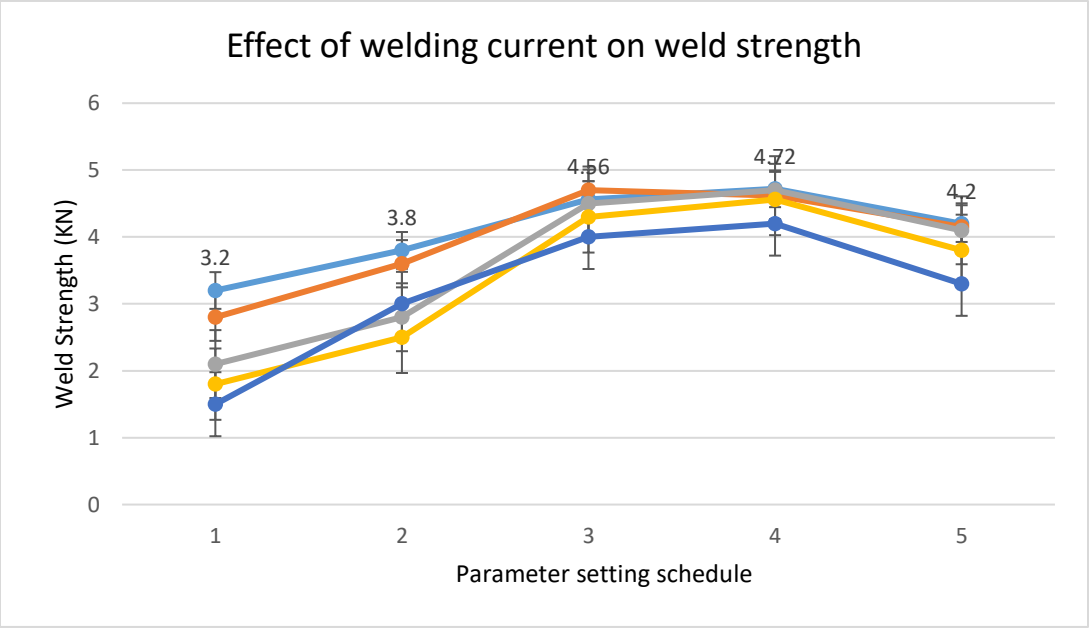

Figure 4.15: The effect of increasing weld time on the strength of the weld

From the figure above, each line plot shows the results of 5 set of specimens for different parameter schedules tested after welding them using different welding parameters with increasing values of the weld time. The values for the different sizes of the nugget diameter are shown in the table below.

Table 4.12: The values of weld strength obtained from the different parameter setting schedules under increasing weld time.

Schedule	Values of weld	Strength	(KN)	
3.2	3.8	4.56	4.72	4.2
2.8	3.6	4.7	4.62	4.15
2.1	2.8	4.5	4.7	4.1
1.8	2.5	4.3	4.56	3.8
1.5	3	4	4.2	3.3

The results show that the maximum value of the weld strength obtained was 4.72 KN corresponding to a welding current of 8A, electrode force of 18kgf and weld time of 30cycles.

CHAPTER FIVE: CONCLUSION AND RECOMMENDATIONS

5.1 Conclusion

The objectives of this study were threefold. Firstly, the investigation aimed to ascertain the impact of parameters on size of the nugget in spot welds obtained through the utilization of an annular recess electrode. Secondly, the study endeavored to analyze the effect of parameters on the overall strength of spot welds produced through application of an annular recess electrode. Lastly, the research aimed to identify and establish optimal parameters that contributed to enhanced strength of resistance spot welds obtained using an annular recess electrode.

The copper electrodes used in this study adhered to the ISO 5182:2008 Standard. The novel electrode has a centrally located hole measuring 6 mm deep and 3 mm in diameter, filled with a heat-resistant mixture of cement, clay, and kaolin. The study investigated how applied electrode force, current and weld time impacted on the integrity of the spot weld produced with an electrode of annular design. The findings indicated that the strength of the weld increased with increasing current and the maximum value of weld strength was achieved when welding current reached 10A. Beyond that current, the quality of the spot weld will be lost. This result was observed in both the destructive and non-destructive tests conducted.

On the side of the weld time, the findings indicated that for both the destructive and non- destructive evaluation, the quality of spot weld increased with increasing current. However, from the two tests, it was observed that although increasing weld time increased the spot weld quality, it was necessary to balance welding current with weld

time. The findings on the effect of electrode force on the spot weld quality indicated that under the non-destructive test there was no significant effect on the quality of the spot weld when electrode force increased. However, the non-destructive evaluation indicated a loss of spot weld quality with increasing electrode force. From the experiments conducted, the optimum spot-welding parameters to produce a quality spot weld were 9A, 30 cycles and 12 kgf.

5.2 Recommendations

The refractory material inserted into the recess hole does not hold in there for a long time. As one continues to spot weld, the refractory materials keep on breaking off or coming out which requires to continuously change the electrode and making the results inconsistent. I recommend more study to be done around this area to ensure that the type of refractory material used sticks inside and the electrode is used for a long time for consistent results.

The range of values used for the parameters during the non-destructive testing was big. Welding current was 7, 10 and 13A, welding time was 10, 20 and 30 cycles and electrode force were 8, 18 and 30Kgf. These values were used for purposes of getting a picture of the effect of varying these parameters on the quality of spot weld. I recommend more tests to be done, on this novel electrode, using a smaller range of values to determine more reliable results.

There is not much study done on the effect of varying these parameters on the microstructure of carbon steel using this novel electrode. I recommend a study to be done around this area of microstructure behavior using this novel electrode.

REFERENCES

Abass, K. I. (2023). The proper electrode geometry of resistance spot welding process. U.P.B. Sci. Bull., Series D, 85(4), ISSN 1454-2358.

Alcantar-Mondragón, N., Reyes-Calderón, F., García-García, V., Garnica-González, P., & Estrada-Hernández, S. (2023). Thermal and diffusion conditions for delta ferrite formation in partially melted and heat-affected zones of multipass SAW joint performed in martensitic stainless steel 12Cr–1Mo. *Results in Materials*, *20*, 100489. https://doi.org/10.1016/j.rinma.2023.100489

Andersson, O. (2013). Process planning of resistance spot welding. Retrieved from https://urn.kb.se/resolve?urn=urn:nbn:se:kth:diva-117807

Azzouzi, D., Benkhedda, Y., & Boumeddane, B. (2019). Parametric study of the nugget growth in spot welding of 304L stainless steel sheets having equal and unequal thicknesses. SN Applied Sciences, 1, 1-12. https://doi.org/10.1007/s42452-019-1502-9

Bamberg, P., Gintrowski, G., Liang, Z., Schiebahn, A., Reisgen, U., Precoma, N., & Geffers, C. (2021). Development of a new approach to resistance spot weld AW-7075 aluminum alloys for structural applications: An experimental study – Part 1. *Journal of Materials Research and Technology*, *15*, 5569-5581. https://doi.org/10.1016/j.jmrt.2021.10.142

Biradar, A. K., & Dabade, B. M. (2020). Optimization of resistance spot welding process parameters in dissimilar joint of MS and ASS 304 sheets. Materials Today:

Proceedings, 26, 1284-1288. https://doi.org/10.1016/j.matpr.2020.02.258

Bowers, R. J., Sorensen, C. D., & Eagar, T. W. (2000). Electrode geometry in resistance spot welding. *Journal of Manufacturing Processes*, *2*(1), 28-41.

BWS. (2019). How to carry out a spot weld peel test. Retrieved December 29, 2023, from https://www.basicwelding.co.uk/blogs/news/how-to-carry-out-a-spot-weld-peel-test

Chang, B. H., & Zhou, Y. (2003). Numerical study on the effect of electrode force in small-scale resistance spot welding. *Journal of Materials Processing Technology*, *139*(1), 635-641. https://doi.org/10.1016/S0924-0136(03)00613-7

Charde, N. (2014). Experimental analysis of spot weld growth on carbon steels using pneumatics-driven 75KVA spot welder. *Journal of Mechanical and Industrial Engineering Research*, 69.

Charde, N., Yusof, F., & Rajkumar, R. (2014). Material characterizations of mild steels, stainless steels, and both steel mixed joints under resistance spot welding (2-mm sheets). *The International Journal of Advanced Manufacturing Technology*, *75*(1), 373-384. https://doi.org/10.1007/s00170-014-6158-z

Chen, N., Wang, H. P., Wang, M., Carlson, B. E., & Sigler, D. R. (2019). Schedule and electrode design for resistance spot weld bonding Al to steels. Journal of Materials Processing Technology, 265, 158-172.

Edwards, K. L. (2004). Strategic substitution of new materials for old: Applications in

automotive product development. *Materials & Design*, *25*(6), 529-533. https://doi.org/10.1016/j.matdes.2003.12.008

Eisazadeh, H., Hamedi, M., & Halvaee, A. (2010). New parametric study of nugget size in resistance spot welding process using finite element method. *Materials & Design*, *31*(1), 149-157. https://doi.org/10.1016/j.matdes.2009.06.042

EXPERIMENTAL analysis of spot weld growth on carbon steels using pneumatics-driven 75KVA spot welder. (2023). *ProQuest*. Retrieved from https://www.proquest.com/openview/e408a11bff77028f19a10f3f2d478dad/1?pq-origsite=gscholar&cbl=2032140

Forster, P. M., Smith, C. J., Walsh, T., Lamb, W. F., Lamboll, R., Hauser, M., Zhai, P., & others. (2023). Indicators of global climate change 2022: Annual update of large-scale indicators of the state of the climate system and human influence. *Earth System Science Data*, 15(6), 2295-2327. Copernicus GmbH. https://doi.org/10.5194/essd-15-2295-2023

Gawai, B., & Sedani, C. M. (2019). Optimization of process parameters for resistance spot welding process of HR E-34 using response surface method: A review. *ResearchGate*. https://doi.org/10.13140/RG.2.2.31190.09283

Ghatei-Kalashami, A., Zhang, S., Shojaee, M., Midawi, A. R. H., Goodwin, F., & Zhou, N. Y. (2022). Failure behavior of resistance spot welded advanced high strength steel: The role of surface condition and initial microstructure. *Journal of Materials Processing Technology*, 299, 117370. Elsevier.

https://doi.org/10.1016/j.jmatprotec.2021.117370

Goodarzi, M., Marashi, S. P. H., & Pouranvari, M. (2009). Dependence of overload performance on weld attributes for resistance spot welded galvanized low carbon steel. *Journal of Materials Processing Technology*, *209*(9), 4379-4384. https://doi.org/10.1016/j.jmatprotec.2008.11.017

Halim, M. F. H. A. (2018). Effect of spot welding processing parameters on ferrous and non-ferrous metal [Unpublished manuscript]. Retrieved from http://eprints.usm.my/53050/1/Effect%20Of%20Spot%20Welding%20Processing%20Parameters%20On%20Ferrous%20And%20Non%20Ferrous%20Metal_Mohd%20Fahmi%20Hafiz%20Abd%20Halim_B1_2018.pdf

Hamzah, M. M., Barrak, O. S., Abdullah, I. T., & Hussein, S. K. (2024). Process parameters influence the mechanical properties and nugget diameter of AISI 316 stainless steel during resistance spot welding. International Journal of Applied Mechanics and Engineering, 29(2), 79-89.

Hassoni, S. M., Barrak, O. S., Ismail, M. I., & Hussein, S. K. (2022). Effect of welding parameters of resistance spot welding on mechanical properties and corrosion resistance of 316L. Materials Research, 25, e20210117.

Huda, N., Nam, D. G., & Park, Y. D. (2019). Study on the mechanism of nugget growth behavior in three sheets stack resistance spot welding. Journal of Welding and Joining, 37 (6), 564–571.

in lightweight production of automotive parts. International Journal of Lightweight Materials and Manufacture , 1 (4), 229–238. doi: 10.1016/j.ijlmm.2018.09.001

Jadhav, S. A., & Venkatesh, D. (2016). A review paper on optimization of process parameter of spot welding by multi-objective Taguchi. *International Research Journal of Engineering and Technology (IRJET)*, 6.

Khader, R., Valappil, A., Murad, M., & Abu Qudeiri, J. (2023). Effect of spot-welding parameters on the strength of the weld of metal sheets. In Proceedings of the International Conference on Industrial Engineering and Operations Management (pp. 7-9). Manila, Philippines: IEOM Society International.

Khuenkaew, T., & Kanlayasiri, K. (2018b). Selection of electrode tips for the resistance spot welding of dissimilar stainless steels. MATEC Web of Conferences, 192, 01007. doi: 10.1051/matecconf/201819201007

Kustroń, P., Korzeniowski, M., Piwowarczyk, T., & Sokołowski, P. (2021). Development of resistance spot welding processes of metal–plastic composites. *Materials*, 14(12), Article 12. https://doi.org/10.3390/ma14123233

Liu, X., Wei, Y., Wu, H., & Zhang, T. (2020). Factor analysis of deformation in resistance spot welding of complex steel sheets based on reverse engineering technology and direct finite element analysis. Journal of Manufacturing Processes, 57, 72-90.

Mashhuriazar, A., Mirsalehi, S. E., & Moradi, K. (2024). An investigation of the effects of parameters on the development of nuggets and the tensile properties of IN-625

during resistance spot welding. Experimental Techniques, 48(4), 735-745. https://doi.org/10.1007/s40799-023-00752-6

Matsukage, T., Sakurai, S., Traui, T., & Iyota, M. (2023). Mechanical properties of resistance-spot-welded joints of aluminum castings and wrought alloys. Engineering Proceedings, 43(1), 52.

Odiaka, T., Akinlabi, S. A., Madushele, N., Fatoba, O. S., Hassan, S., & Akinlabi, E. T. (2021). Statistical analysis of the effect of welding parameters on the tensile strength of titanium reinforced mild steel joints using Taguchi's DoE. Materials Today: Proceedings, 44, 1202-1206. Indore, India: 11th International Conference on Materials Processing and Characterization.

Perulli, P., Dassisti, M., & Casalino, G. (2020). Thermo-mechanical simulation of hybrid welding of DP/AISI 316 and TWIP/AISI 316 dissimilar weld. *Journal of Applied Physics*, 9.

Pouranvari, M., Asgari, H. R., Mosavizadch, S. M., Marashi, P. H., & Goodarzi, M. (2007). Effect of weld nugget size on overload failure mode of resistance spot welds. *Science and Technology of Welding and Joining*, *12*(3), 217-225. https://doi.org/10.1179/174329307X164409

Qiu, R., Li, J., Shi, H., & Yu, H. (2023). Characterization of resistance spot welded joints between aluminum alloy and mild steel with composite electrodes. Journal of Materials Research and Technology, 24, 1190-1202.

Rawal, M., Kolhapure, R., Sutar, S., & Shinde, V. (2016, October). Optimization of resistance spot welding of 304 steel using GRA. *International Journal of Computer Engineering in Research Trends*, 3, 492-499. https://doi.org/10.22362/ijcert/2016/v3/i9/48869

Rawal, M., Kolhapure, R., Sutar, S., & Shinde, V. (2016, October). Optimization of resistance spot welding of 304 steel using gra. International Journal of Computer Engineering In Research Trends , 3 , 492–499. doi: 10.22362/ijcert/2016/v3/i9/48869

Reddy Gillela, J., Jaidi, V., & Gude, J. (2023). A numerical study on contact conditions, dynamic resistance, and nugget size of resistance spot weld joints of AISI 1008 steel sheets. *Numerical Heat Transfer Part-A*, 84.

Ren, D., Zhao, D., Zhao, K., Liu, L., & He, Z. (2019). Resistance ceramic-filled annular welding of dp980 high-strength steel. Materials & Design, 183, 108118. Retrieved from https://doi.org/10.1016/j.matdes.2019.108118 doi: 10.1016/j.matdes.2019.108118

SA Jadhav, D. V. (2016). A review paper on optimization of process parameter of spot welding by multi-objective taguchi. International Research Journal of Engineering and Technology (IRJET), 6.

Senkara, J., Zhang, H., & Hu, S. J. (2004). Expulsion prediction in resistance spot welding. *Welding Journal*.

Shawon, M. R. A. (2014). Investigation into physical and mechanical properties and

failure mode of resistance spot welded dissimilar metal joints. *Engineering, Materials Science*.

Tanmoy, D. (2022). Resistance spot welding: Principles and its applications. In *Engineering Principles-Welding and Residual Stresses*. Intech Open. https://doi.org/10.5772/intechopen.100201

Taufiqurrahman, I., Ahmad, A., Mustapha, M., Ginta, T. L., Haryoko, L. A. F., & Shozib, I. A. (2021). The effect of welding current and electrode force on the heat input, weld diameter, and physical and mechanical properties of SS316L/Ti6Al4V dissimilar resistance spot welding with aluminum interlayer. Materials, 14(5), 1129. https://doi.org/10.3390/ma14051129

Taylor, G. A., Sun, X., & Khaleel, M. A. (2007). Effect of weld nugget size on overload failure mode of resistance spot welds. *Science and Technology of Welding and Joining*, 12(3). Taylor & Francis. https://www.tandfonline.com/doi/abs/10.1179/174329307X164409

Tisza, M., & Czinege, I. (2018). Comparative study of the application of steels and aluminium in lightweight production of automotive parts. *International Journal of Lightweight Materials and Manufacture*, 1(4), 229-238. Elsevier. https://doi.org/10.1016/j.ijlmm.2018.09.001

Vishwakarma, S. K., Shrivastava, A., & Singh, S. (2018). Optimization of resistance spotwelding parameters using taguchi method. International Journal of Emerging Research in Management and Technology, 6(7), 196. doi: 10.23956/ijermt.v6i7.211

Watmon, T. B., Wandera, C., & Apora, J. (2020). Characteristics of resistance spot welding using annular recess electrodes. Retrieved from https://doi.org/10.1016/j.jajp.2020.100035 doi: 10.1016/j.jajp.2020.100035

Wohner, M., Mitzschke, N., & Jüttner, S. (2021). Resistance spot welding with variable electrode force—development and benefit of a force profile to extend the weldability of 22MnB5+AS150. Weld World, 65, 105-117. https://doi.org/10.1007/s40194-020-01001-2

Xia, Y. J., Su, Z. W., Li, Y. B., Zhou, L., & Shen, Y. (2019). Online quantitative evaluation of expulsion in resistance spot welding. Journal of Manufacturing Processes, 46, 34-43.

Yang, K., El-Sari, B., Olfert, V., Wang, Z., Biegler, M., Rethmeier, M., & Meschut, G. (2024). Expulsion prevention in resistance spot welding of dissimilar joints with ultra-high strength steel: An analysis of the mechanism and effect of preheating current. Journal of Manufacturing Processes, 124, 489-502.

Zhao, H., Yan, N., Xing, Z., Chen, L., & Jiang, L. (2020). Thermal calculation and experimental investigation of electric heating and solid thermal storage system. Energies, 13, 5241. https://doi.org/10.3390/en13205241

Zhou, K., & Cai, L. (2014). Study on effect of electrode force on resistance spot welding process. *Journal of Applied Physics*, 8.

Appendix A: Full Annular Recess Electrode Design

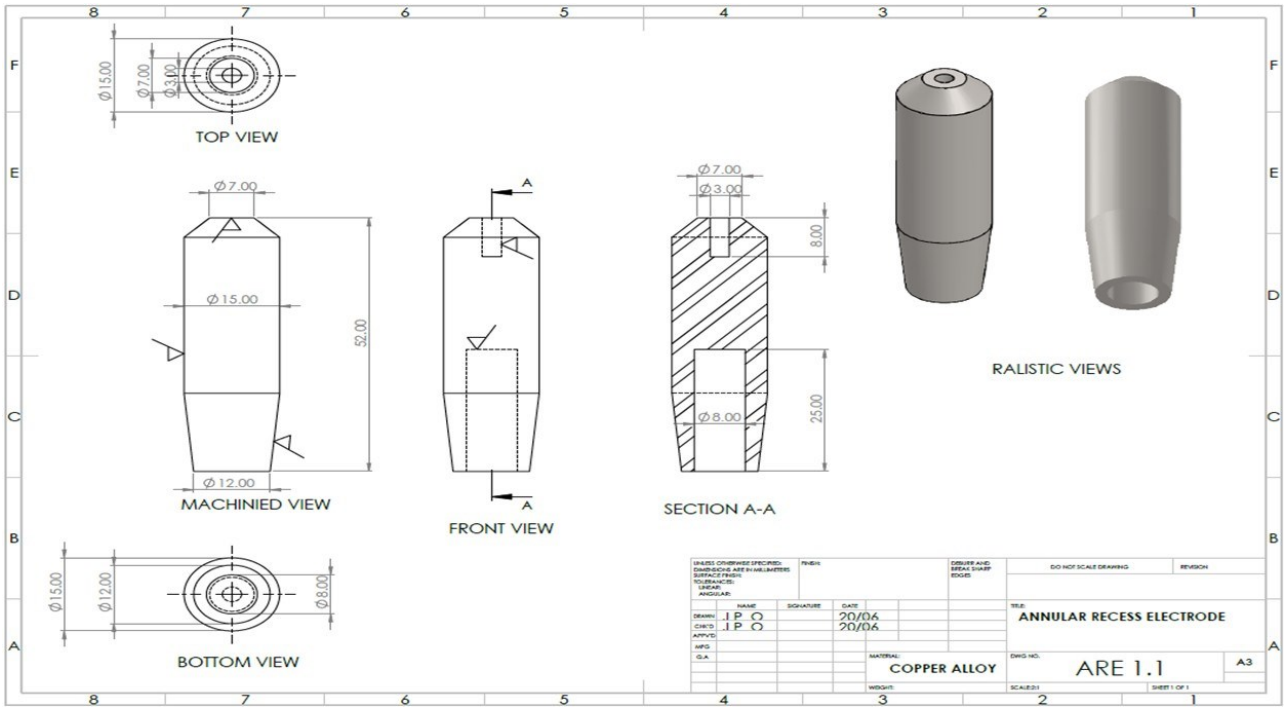

Figure A.1: Drawings for the design of the annular recess electrode

Specimen	Welding current (A)	Electrode Force (Kgf)	Weld Time (Cycles)	Weld strength (KN)	Nugget Diameter (mm)
1	6	8	10	3.2	6.2
	6	12	15	3.8	6.4
3	6	18	20	4.56	6.3
4	6	24	25	4.68	6.4
5	6	30	30	4.2	6.2
6	7	8	10	2.8	6.3
7	7	12	15	3.6	6.5
8	7	18	20	4.5	6.5
9	7	24	25	4.62	6.4
10	7	30	30	4.15	6.1
11	8	8	10	2.1	6.7
12	8	12	15	2.8	6.7
13	8	18	20	4.5	6.9
14	8	24	25	4.7	6.9
15	8	30	30	4.1	6.4
16	9	8	10	1.8	6.8
17	9	12	15	2.5	6.9
18	9	18	20	4.3	7.1
19	9	24	25	4.4	7.15
20	9	30	30	3.8	7
21	10	8	10	1.5	6.9
22	10	12	15	3	7
23	10	18	20	4	7.2
24	10	24	25	4.2	7.1
25	10	30	30	3.3	6.8

Table A1: Orthogonal Array for Evaluating the Effect of Welding Current on the Quality of Spot Weld.

Specimen	Weld Time (Cycles)	Electrode Force (Kgf)	Welding Current (A)	Weld Strength (KN)	Nugget diameter (mm)
1	10	8	6	1.5	6.2
2	10	1	7	1.8	6.3
3	10	1	8	2.3	6.7
4	10	2	9	2.5	6.8
5	10	3	10	2	6.7
6	15	8	6	2.15	6.4
7	15	1	7	2.8	6.5
8	15	1	8	3.1	6.7
9	15	2	9	3.65	6.9
10	15	3	10	3	7.2
11	20	8	6	3.5	6.1
12	20	1	7	4.45	6.2
13	20	1	8	4.4	6.9
14	20	2	9	4.65	7.2
15	20	3	10	3.7	7
16	25	8	6	3.5	6.4
17	25	1	7	4.45	6.4
18	25	1	8	4.4	6.9
19	25	2	9	4.65	7.2
20	25	3	10	3.7	7
21	30	8	6	3.8	6.5
22	30	1	7	4	6.6
23	30	1	8	4.72	7
24	30	2	9	4.5	7
25	30	3	10	4	6.8

Table A2: Orthogonal Array for evaluating the effect of weld time on the quality of spot weld

Specim	Electrode Force	Welding current	Weld Time	Weld strength	Nugget Diameter (mm)
1	8	6	1	4.15	6.8
2	8	7	1	4.42	6.8
3	8	8	2	4	6.9
4	8	9	2	3.5	6.5
5	8	1	3	1.8	6
6	1	6	1	3.85	6.5
7	1	7	1	4.25	6.8
8	1	8	2	4.5	6.2
9	1	9	2	3.8	6
10	1	1	3	2.6	5.3
11	1	6	1	3.65	6
12	1	7	1	4	6.8
13	1	8	2	3.8	5.8
14	1	9	2	2.5	5
15	1	1	3	2	4.6
16	2	6	1	3.45	5.2
17	2	7	1	3.65	5.9
18	2	8	2	3.5	5.2
19	2	9	2	2.8	4.5
20	2	1	3	2.5	4
21	3	6	1	3.25	5
22	3	7	1	3.3	5.4
23	3	8	2	3.2	4.5
24	3	9	2	3	4
25	3	1	3	2.8	3.8

Table A3: Orthogonal Array for evaluating the effect of electrode force on the quality of spot weld

Appendix B: Mass SpectrometerTest

SPECTRO Sample Results

Sample Result Name	Type	Measure Date Time	Recalculation Date Time
MILD STEEL/KENNETH/A	Unknown	10 October 2020	13:03:39
Origin	**Method Name**	**Method Version**	**Operator Name**
Measured	Fe-01-M...		
Check Type	**Check Status**	**Grade Verification Name**	**Grade Verification Similarity**
None	Not Used		0
Correction Type	**Type Corr Sample Name**	**Grade Search Name**	**Grade Search Similarity**
None			0
Type	**Status**	**Outlier Removal**	
None	Not Used		
Sample Name	**Analyst**	**Shift**	
MILD STEEL	KENNETH	A	

	C Conc %	Si Conc %	Mn Conc %	P Conc %	S Conc %	Cr Conc %	Mo Conc %	Ni Conc %	Al Conc %	Co Conc %	Cu Conc %	Nb Conc %	Ti Conc %
1	**0.021**	**0.007**	**0.13**	**0.006**	**0.002**	**0.017**	**<0.0010**	**0.007**	**0.060**	**0.003**	**0.006**	**<0.004**	**<0.0010**
2	**0.026**	**0.010**	**0.19**	**0.010**	**0.004**	**0.025**	**0.001**	**0.011**	**0.059**	**0.005**	**0.008**	**<0.004**	**<0.0010**
3	**0.028**	**0.013**	**0.22**	**0.013**	**0.004**	**0.028**	**0.002**	**0.012**	**0.068**	**0.005**	**0.009**	**<0.004**	**<0.0010**
Min Cal	0.002	0.005	0.0005	0.0005	0.0002	0.0005	0.0010	0.002	0.0005	0.002	0.0005	0.004	0.0010
Rep	0.025	0.010	0.18	0.009	0.003	0.023	0.001	0.010	0.062	0.004	0.007	<0.004	<0.0010
Max Cal	4.35	18.00	20.00	2.40	0.43	32.00	9.50	43.50	2.80	21.00	8.00	3.00	3.20
Mean	**0.025**	**0.010**	**0.18**	**0.009**	**0.003**	**0.023**	**0.001**	**0.010**	**0.062**	**0.004**	**0.007**	<-0.005	<-0.002
SD	0.004	0.003	0.042	0.003	0.0009	0.005	0.0004	0.002	0.005	0.0008	0.002	0.0000	0.0000
RSD	16.16	29.48	23.13	37.43	28.30	23.01	29.87	23.57	8.30	18.68	22.31	0.0000	0.0000

	V Conc %	W Conc %	Pb Conc %	Sn Conc %	Mg Conc %	As Conc %	Zr Conc %	Bi Conc %	Ca Conc %	Ce Conc %	Sb Conc %	Se Conc %	Te Conc %
1	**<0.0005**	**0.014**	**0.002**	**0.001**	**<0.0010**	**<0.002**	**<0.002**	**<0.002**	**0.0004**	**0.004**	**<0.002**	**<0.001**	**0.001**
2	**<0.0005**	**<0.007**	**<0.002**	**0.002**	**<0.0010**	**<0.002**	**<0.002**	**<0.002**	**0.0005**	**<0.002**	**<0.002**	**<0.001**	**<0.0010**
3	**<0.0005**	**<0.007**	**<0.002**	**0.001**	**<0.0010**	**<0.002**	**<0.002**	**<0.002**	**0.001**	**<0.002**	**<0.002**	**<0.001**	**<0.0010**
Min Cal	0.0005	0.007	0.002	0.0005	0.0010	0.002	0.002	0.002	0.0001	0.002	0.002	0.001	0.0010
Rep	<0.0005	0.009	0.002	0.001	<0.0010	<0.002	<0.002	<0.002	0.0007	0.002	<0.002	<0.001	0.001
Max Cal	10.00	20.50	0.38	0.24	0.23	0.20	0.23	0.036	0.013	0.54	0.24	0.30	0.080
Mean	<-0.0008	<0.003	<-0.0001	**0.001**	<-0.001	<-0.001	<0.0001	<-0.003	**0.0007**	<0.0007	<0.0008	<-0.004	<0.0009
SD	0.0000	0.004	0.0001	0.0001	0.0000	0.0000	0.0000	0.0000	0.0004	0.002	0.0000	0.0000	0.0000
RSD	0.0000	43.53	2.80	8.64	0.0000	0.0000	0.0000	0.0000	57.2	63.9	0.0000	0.0000	1.37

	Ta Conc %	B Conc %	Zn Conc %	La Conc %	N Conc %	Fe Conc %
1	**0.094**	**0.0006**	O 0.045!	**0.014**	**0.024**	**99.5**
2	**0.046**	**0.0008**	O 0.045!	**0.006**	**0.021**	**99.5**
3	**<0.020**	**0.0007**	**>0.045**	**0.002**	**0.021**	**99.5**
Min Cal	0.020	0.0002	0.0005	0.0005	0.0010	
Rep	0.053	0.0007	O 0.045!	0.007	0.022	99.5
Max Cal	0.76	0.11	0.045	0.22	0.50	
Mean	**0.046**	**0.0007**	O 20.46!	**0.007**	**0.022**	**79.1**
SD	0.037	0.0001	0.0000	0.006	0.002	18.57
RSD	70.5	11.78	0.0000	81.2	7.27	18.66

Figure B.1:Results of the first Mass Spectrometer Test for the Composition of the Material

SPECTRO

Sample Results

Sample Result Name	Type	Measure Date Time	Recalculation Date Time
MF-KYU-M001-2/KENNETH/A	Unknown	17 October 2020	11:23:00
Origin	**Method Name**	**Method Version**	**Operator Name**
Measured	Fe-01-M		
Check Type	**Check Status**	**Grade Verification Name**	**Grade Verification Similarity**
None	Not Used		0
Correction Type	**Type Corr Sample Name**	**Grade Search Name**	**Grade Search Similarity**
None			0
Type	**Status**	**Outlier Removal**	
Grade	Not Used		
Sample Name	**Analyst**	**Shift**	
MF-KYU-M001-2	KENNETH	A	

	C Conc %	Si Conc %	Mn Conc %	P Conc %	S Conc %	Cr Conc %	Mo Conc %	Ni Conc %	Al Conc %	Co Conc %	Cu Conc %	Nb Conc %	Ti Conc %
1	**0.024**	**0.010**	**0.23**	**0.021**	**0.006**	**0.030**	**0.002**	**0.013**	**0.065**	**0.006**	**0.009**	**<0.004**	**<0.0010**
2	**0.023**	**0.011**	**0.23**	**0.021**	**0.005**	**0.032**	**0.002**	**0.014**	**0.062**	**0.006**	**0.010**	**<0.004**	**<0.0010**
Min Cal	0.002	0.005	0.0005	0.0005	0.0002	0.0005	0.0010	0.002	0.0005	0.002	0.0005	0.004	0.0010
Rep	0.023	0.011	0.23	0.021	0.006	0.031	0.002	0.013	0.063	0.006	0.010	<0.004	<0.0010
Max Cal	4.35	18.00	20.00	2.40	0.43	32.00	9.50	43.50	2.80	21.00	8.00	3.00	3.20
Mean	**0.023**	**0.011**	**0.23**	**0.021**	**0.006**	**0.031**	**0.002**	**0.013**	**0.063**	**0.006**	**0.010**	<-0.006	<-0.004
SD	0.0007	0.0009	0.002	0.0003	0.0006	0.001	0.0003	0.0007	0.002	0.0002	0.0003	0.0000	0.0000
RSD	2.87	8.25	0.79	1.23	9.80	3.75	14.14	5.24	3.43	3.30	2.85	0.0000	0.0000

	V Conc %	W Conc %	Pb Conc %	Sn Conc %	Mg Conc %	As Conc %	Zr Conc %	Bi Conc %	Ca Conc %	Ce Conc %	Sb Conc %	Se Conc %	Te Conc %
1	**<0.0005**	**<0.007**	**<0.002**	**0.001**	**<0.0010**	**<0.002**	**<0.002**	**<0.002**	**0.0004**	**<0.002**	**0.006**	**0.003**	**0.002**
2	**<0.0005**	**<0.007**	**<0.002**	**0.001**	**<0.0010**	**<0.002**	**<0.002**	**<0.002**	**0.0003**	**<0.002**	**0.006**	**0.004**	**0.002**
Min Cal	0.0005	0.007	0.002	0.0005	0.0010	0.002	0.002	0.002	0.0001	0.002	0.002	0.001	0.0010
Rep	<0.0005	<0.007	<0.002	0.001	<0.0010	<0.002	<0.002	<0.002	0.0004	<0.002	0.006	0.003	0.002
Max Cal	10.00	20.50	0.38	0.24	0.23	0.20	0.23	0.036	0.013	0.54	0.24	0.30	0.080
Mean	<-0.001	<-0.009	<-0.002	**0.001**	<-0.003	<0.0000	<0.0000	<-0.005	**0.0004**	<-0.003	**0.006**	**0.003**	**0.002**
SD	0.0000	0.0000	0.0000	0.0001	0.0000	0.0000	0.0000	0.0000	0.0000	0.0000	0.0000	0.0002	0.0002
RSD	0.0000	0.0000	0.0000	8.09	0.0000	0.0000	0.0000	0.0000	11.53	0.0000	0.003	6.16	10.79

	Ta Conc %	B Conc %	Zn Conc %	La Conc %	N Conc %	Fe Conc %
1	**<0.020**	**0.001**	**>0.045**	**<0.0005**	**0.017**	**99.5**
2	**<0.020**	**0.001**	**0.003**	**<0.0005**	**0.014**	**99.5**
Min Cal	0.020	0.0002	0.0005	0.0005	0.0010	
Rep	<0.020	0.001	0.024	<0.0005	0.016	99.5
Max Cal	0.76	0.11	0.045	0.22	0.50	
Mean	<-0.013	**0.001**	**0.031**	<-0.0010	**0.016**	**99.6**
SD	0.0000	0.0002	0.030	0.0000	0.002	0.032
RSD	0.0000	15.62	124	0.0000	14.18	0.032

Figure B.2: Results of the Second Mass Spectrometer Test for the Composition of the Material

SPECTRO

Sample Results

Sample Result Name	Type	Measure Date Time	Recalculation Date Time
MF-KYU-M001-2/KENNETH/A	Unknown	17 October 2020	11:20:33
Origin	**Method Name**	**Method Version**	**Operator Name**
Measured	Fe-01-M		
Check Type	**Check Status**	**Grade Verification Name**	**Grade Verification Similarity**
None	Not Used		0
Correction Type	**Type Corr Sample Name**	**Grade Search Name**	**Grade Search Similarity**
None			0
Type	**Status**	**Outlier Removal**	
None	Not Used		
Sample Name	**Analyst**	**Shift**	
MF-KYU-M001-2	KENNETH	A	

	C Conc %	Si Conc %	Mn Conc %	P Conc %	S Conc %	Cr Conc %	Mo Conc %	Ni Conc %	Al Conc %	Co Conc %	Cu Conc %	Nb Conc %	Ti Conc %
1	**0.027**	**0.011**	**0.23**	**0.019**	**0.005**	**0.032**	**0.002**	**0.013**	**0.10**	**0.007**	**0.010**	**<0.004**	**<0.0010**
2	**0.021**	**0.012**	**0.23**	**0.020**	**0.005**	**0.031**	**0.002**	**0.013**	**0.062**	**0.006**	**0.010**	**<0.004**	**<0.0010**
Min Cal	0.002	0.005	0.0005	0.0005	0.0002	0.0005	0.0010	0.002	0.0005	0.002	0.0005	0.004	0.0010
Rep	0.024	0.011	0.23	0.019	0.005	0.031	0.002	0.013	0.081	0.006	0.010	<0.004	<0.0010
Max Cal	4.35	18.00	20.00	2.40	0.43	32.00	9.50	43.50	2.80	21.00	8.00	3.00	3.20
Mean	**0.024**	**0.011**	**0.23**	**0.019**	**0.005**	**0.031**	**0.002**	**0.013**	**0.081**	**0.006**	**0.010**	<-0.005	<-0.004
SD	0.005	0.0001	0.0003	0.0007	0.0003	0.0006	0.0000	0.0002	0.027	0.0008	0.0003	0.0000	0.0000
RSD	19.80	0.76	0.13	3.50	5.78	1.85	1.96	1.16	33.05	12.96	3.26	0.0000	0.0000

	V Conc %	W Conc %	Pb Conc %	Sn Conc %	Mg Conc %	As Conc %	Zr Conc %	Bi Conc %	Ca Conc %	Ce Conc %	Sb Conc %	Se Conc %	Te Conc %
1	**<0.0005**	**<0.007**	**<0.002**	**0.002**	**<0.0010**	**<0.002**	**<0.002**	**<0.002**	**0.0005**	**<0.002**	**0.006**	**0.003**	**0.002**
2	**<0.0005**	**<0.007**	**<0.002**	**0.001**	**<0.0010**	**<0.002**	**<0.002**	**<0.002**	**0.0004**	**<0.002**	**0.005**	**0.003**	**0.002**
Min Cal	0.0005	0.007	0.002	0.0005	0.0010	0.002	0.002	0.002	0.0001	0.002	0.002	0.001	0.0010
Rep	<0.0005	<0.007	<0.002	0.002	<0.0010	<0.002	<0.002	<0.002	0.0004	<0.002	0.005	0.003	0.002
Max Cal	10.00	20.50	0.38	0.24	0.23	0.20	0.23	0.036	0.013	0.54	0.24	0.30	0.080
Mean	<-0.001	<-0.009	<-0.002	**0.002**	<-0.002	<-0.001	<0.0000	<-0.005	**0.0004**	<-0.003	**0.005**	**0.003**	**0.002**
SD	0.0000	0.0000	0.0000	0.0002	0.0000	0.0000	0.0000	0.0000	0.0001	0.0000	0.0007	0.0000	0.0000
RSD	0.0000	0.0000	0.0000	11.17	0.0000	0.0000	0.0000	0.0000	16.38	0.0000	13.59	1.57	0.20

	Ta Conc %	B Conc %	Zn Conc %	La Conc %	N Conc %	Fe Conc %
1	**<0.020**	**0.001**	**0.028**	**<0.0005**	**0.022**	**99.4**
2	**<0.020**	**0.0008**	**0.008**	**<0.0005**	**0.015**	**99.5**
Min Cal	0.020	0.0002	0.0005	0.0005	0.0010	
Rep	<0.020	0.001	0.018	<0.0005	0.018	99.5
Max Cal	0.76	0.11	0.045	0.22	0.50	
Mean	<-0.009	**0.001**	**0.018**	<-0.0010	**0.018**	**99.6**
SD	0.0000	0.0004	0.014	0.0000	0.005	0.054
RSD	0.0000	38.40	80.7	0.0000	27.88	0.054

Figure B.3: Results of the Third Mass Spectrometer test for the composition of the Material.

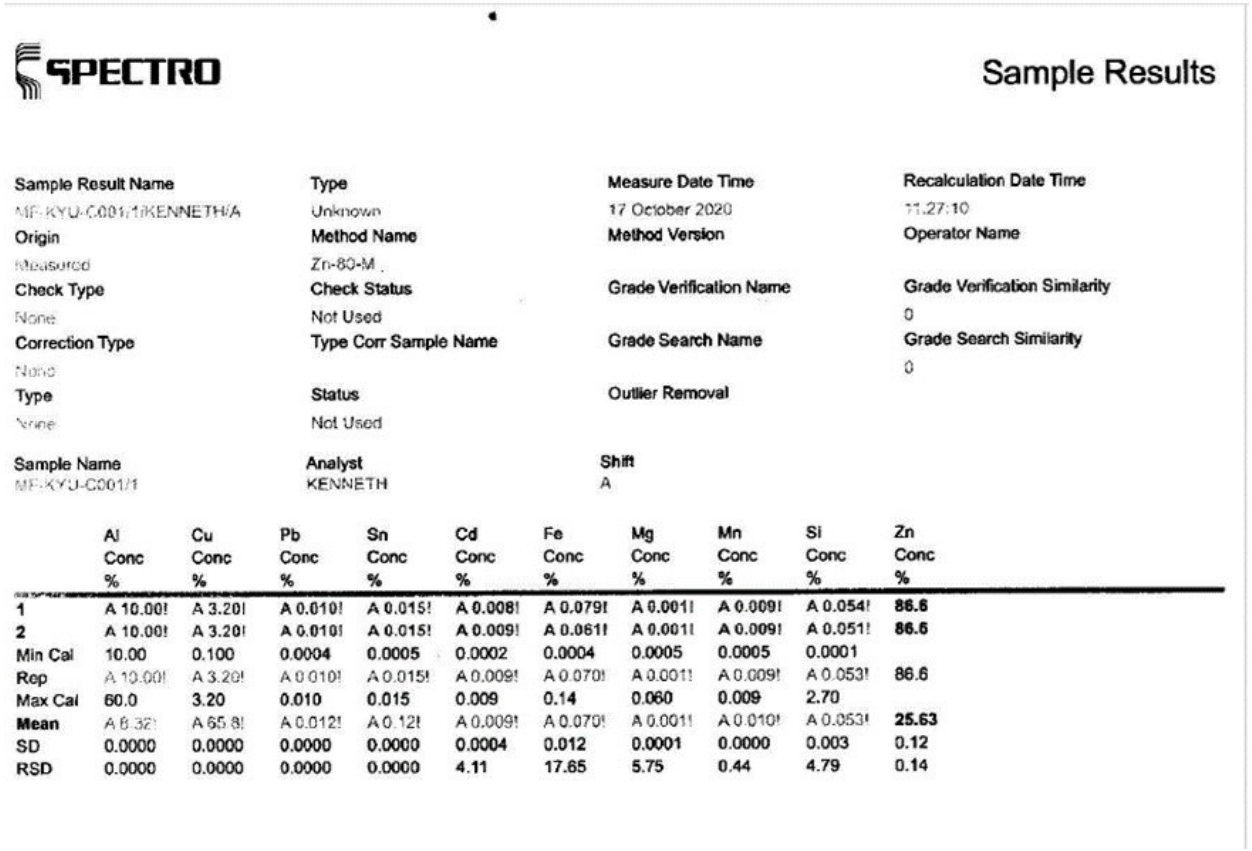

SPECTRO

Sample Results

Sample Result Name	Type	Measure Date Time	Recalculation Date Time
MF-KYU-C001/1/KENNETH/A	Unknown	17 October 2020	11:27:10
Origin	**Method Name**	**Method Version**	**Operator Name**
Measured	Zn-80-M		
Check Type	**Check Status**	**Grade Verification Name**	**Grade Verification Similarity**
None	Not Used		0
Correction Type	**Type Corr Sample Name**	**Grade Search Name**	**Grade Search Similarity**
None			0
Type	**Status**	**Outlier Removal**	
None	Not Used		

Sample Name	Analyst	Shift
MF-KYU-C001/1	KENNETH	A

	Al Conc %	Cu Conc %	Pb Conc %	Sn Conc %	Cd Conc %	Fe Conc %	Mg Conc %	Mn Conc %	Si Conc %	Zn Conc %
1	A 10.00!	A 3.20!	A 0.010!	A 0.015!	A 0.008!	A 0.079!	A 0.001!	A 0.009!	A 0.054!	**86.6**
2	A 10.00!	A 3.20!	A 0.010!	A 0.015!	A 0.009!	A 0.061!	A 0.001!	A 0.009!	A 0.051!	**86.6**
Min Cal	10.00	0.100	0.0004	0.0005	0.0002	0.0004	0.0005	0.0005	0.0001	
Rep	A 10.00!	A 3.20!	A 0.010!	A 0.015!	A 0.009!	A 0.070!	A 0.001!	A 0.009!	A 0.053!	**86.6**
Max Cal	60.0	3.20	0.010	0.015	0.009	0.14	0.060	0.009	2.70	
Mean	A 6.32!	A 65.8!	A 0.012!	A 0.12!	A 0.009!	A 0.070!	A 0.001!	A 0.010!	A 0.053!	**25.63**
SD	0.0000	0.0000	0.0000	0.0000	0.0004	0.012	0.0001	0.0000	0.003	0.12
RSD	0.0000	0.0000	0.0000	0.0000	4.11	17.65	5.75	0.44	4.79	0.14

Figure B.4: Results of the Fourth Mass Spectrometer test for the composition of the test piece.

Appendix C: Introductory Letters

KYAMBOGO UNIVERSITY

P.O. BOX 1 KYAMBOGO, KAMPALA-UGANDA
Tel: 0414 -285001 / 580320
E-mail: mechanical@kyu.ac.ug
www. Kyu.ac.ug
Department of Mechanical and Production Engineering

8th September 2020

The
Plant Manager
Roofing Group Ltd
Namanve Industrial Park

Thru
The Human Resource Manager
Roofing Group Ltd
Namanve

Dear Sir / Madam

RE: **GRADUATE STUDENT RESEARCH PROJECT**

I am obliged to write to you at this moment regarding the above referenced caption. The Department of Mechanical & Production Engineering of Kyambogo University runs a Master of Science Degree Programme in Advanced Manufacturing Systems Engineering. One of the requirements for an Award of the Degree is for the student to conduct an Industrial Project which has a contribution to knowledge and Industry / the Company.

Sir / Madam, the bearer of this note **(Mr. Mwanga Godfrey Fred)** is in the final year pursuing the MSc in AMSE here. His topic for Research is **Performance Optimization of Resistance Spot Welding Electrode with Annular Recess Design**. Thus, your organization was identified as suitable for his research. We therefore, kindly request you to assist him and grant him permission to do his research with you.

On behalf of the Department of Mechanical and Graduate School of Kyambogo University, I wish to inform you that this research is purely for academic purposes and the student is under strict rules to keep all information about your Company that he might come across confidential. In case you have any query, feel free to contact me the undersigned.

Thank you

Yours Sincerely
Dr. Titus Bitek Watmon
Head of Department
Mechanical and Production Engineering
Email. twatmon@kyu.ac.ug
+256 784 111 862

DEPARTMENT OF MECHANICAL AND PRODUCTION ENGINEERING
KYAMBOGO UNIVERSITY
08 SEP 2020
P. O. BOX 1 KYAMBOGO

For approval
10/9/20

Cc: Dean Graduate School. Dean of Faculty of Engineering, Mr. Mwanga Godfrey Fred, Project Coordinator, File

Figure C.1: Request for Permission to Carryout Research work at Roofings Ltd.

ROOFINGS

RRM

MR. MUWANGA GODFREY FRED,
Department of Mechanical & Production Engineering,
Kyambogo University,
Kampala, Uganda

Saturday 12th September,2020

Dear Fred,

RE: PERMISSION TO CONDUCT RESEARCH AT RRM PLANT

The above matter refers.

Ms. Roofings Rolling Mills Limited is in receipt of a communication from your end, requesting for an opportunity to conduct research at our plant ***i.e. "Performance Optimization of Resistance Spot Welding Electrode with Annular Recess Design".*** A copy of the recommendation letter from Kyambogo University dated Tuesday 8th September,2020 is enclosed for your kind perusal and consideration.

To that end, we are pleased to inform you that RRM Management agrees to your request and has accordingly granted you permission to conduct the above mentioned research, in a period of **Two (02) Months** effective **Thursday 1st October, 2020** at no cost implication to Ms. Roofings Rolling Mills Limited.

While conducting your research, you are expected to adhere to set Policies & Procedures in addition to handling all matters with utmost confidentiality. As a researcher you shall not disclose or publish any trade secrets or confidential information pertaining to the business of the company to any person or authority during performance of your research or thereafter. The company reserves the right to take appropriate legal action in the event of breach of this undertaking.

For Ms. Roofings Rolling Mills Limited,

ROOFINGS ROLLING MILLS LTD P.O. BOX 35086, KAMPALA

SHEIKH ARIF
DIRECTOR – TECHNICAL

CC: HUMAN RESOURCE MANAGER
CC: RRM PLANT MANAGERS
CC: HOD, MECHANICAL & PRODUCTION ENGINEERING, KYAMBOGO UNIVERSITY

Figure C.2: Permission to Carryout Research work at Roofings Ltd.tion

Appendix D: Plagiarism Summary Report

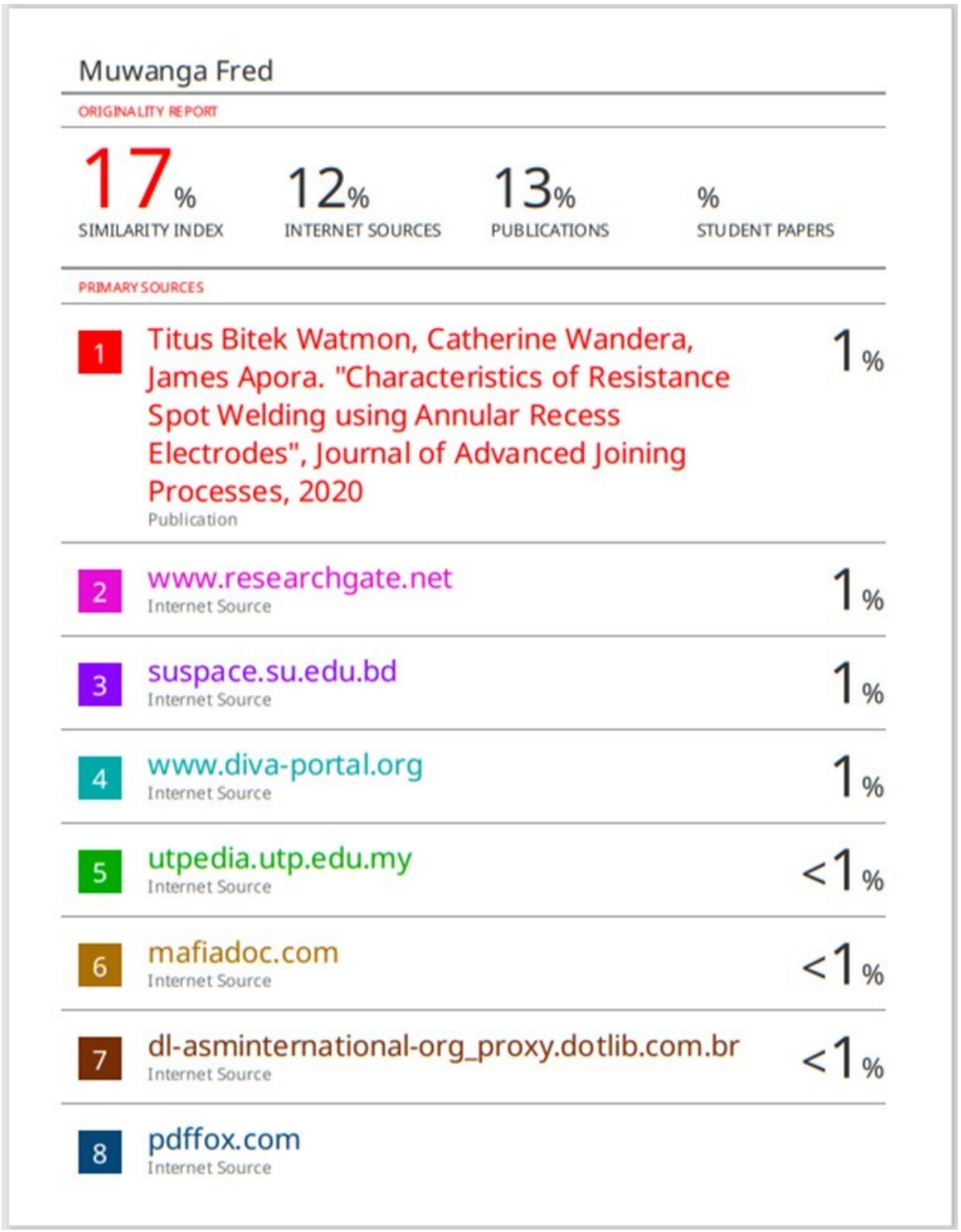

Figure C.1: Plagiarism Summary Report